Geochemical modeling of basic pegmatites from Foz do Iguaçu in the Itaipu region, western Paraná, Brazil

Modelagem geoquímica de pegmatitos básicos em Foz do Iguaçu, região de Itaipu, oeste do Paraná, Brasil

Bruno Titon[1] , Eleonora Maria Gouvêa Vasconcellos[1] , Otávio Augusto Boni Licht[1] , Andrea Marzoli[2]

[1]Universidade Federal do Paraná, Departamento de Geologia, Avenida Cel. Francisco H. dos Santos, 210, Jardim das Américas, CEP: 81530-900, Curitiba, PR, BR (titon@ufpr.br; eleonora@ufpr.br; otavio.licht@gmail.com)
[2]Università degli Studi di Padova, Dipartimento TESAF, Legnaro, Padova, IT (andrea.marzoli@unipd.it)

Abstract

In the westernmost portion of the state of Paraná, in the city of Foz do Iguaçu, basic pegmatites occur within inflated *pahoehoe* basaltic flows of the Paraná Igneous Province. Both rock groups are composed of similar mineral assemblages which include labradorite, augite, ilmenite and titano-magnetite, but pegmatites are medium to coarse grained, whereas basalts are fine grained. Host rocks are geochemically classified as basalts (*s.s.*), while pegmatitic segregations are basaltic andesite and basaltic trachy-andesite, according to the TAS [$(Na_2O + K_2O)$ x SiO_2] diagram. Based on the AFM [$(Na_2O + K_2O) - (FeO_{tot}) - (MgO)$] diagram, all rocks are included in the tholeiitic series, classified as high-Fe tholeiite basalts in the cation plot [Al x (Fe_{tot} + Ti) x Mg]. Variation diagrams indicate enrichment of SiO_2, TiO_2, FeO, Na_2O, K_2O e P_2O_5 coupled with depletion of Al_2O_3, MgO e CaO from basalts to pegmatites. La/Lu_N ratios range between 5.4 to 6.5 for basalts and 6.3 to 7.9 for pegmatites reflecting a greater degree of fractionation in the pegmatitic segregations and, therefore, their more evolved character. Plagioclase crystals in pegmatites have higher sodic contents when compared to those found in host basalts, while CaO content in basaltic pyroxenes is higher than those from pegmatitic segregations. Trace element geochemical modeling results show that it is possible to generate basic pegmatites from basalts comprised of 55 wt.% plagioclase, 35 wt.% clinopyroxene and 10 wt.% titanium and iron oxides. The process occurs as fractional crystallization with 50% residual melt.

Keywords: Paraná Igneous Province; Basaltic flows; Lithogeochemistry; Fractional crystallization; Trace elements.

Resumo

No município de Foz do Iguaçu, Paraná, na região da barragem de Itaipu, ocorrem pegmatitos básicos hospedados em derrames basálticos do tipo *pahoehoe* inflados, da Província Ígnea do Paraná. Ambos os grupos de rochas são constituídos principalmente por labradorita, augita, ilmenita, titano-magnetita; os pegmatitos têm granulação média a grossa, enquanto os basaltos são de granulação fina. As rochas hospedeiras são classificadas geoquimicamente como basaltos e segregações pegmatíticas são andesi-basaltos e traquibasaltos, segundo o diagrama TAS [(Na_2O+K_2O) x SiO_2]. As rochas agrupam-se no campo da série toleítica, de acordo com o diagrama AFM [$(Na_2O+K_2O) - (FeO_{tot}) - (MgO)$], sendo classificadas como basaltos toleíticos de alto-Fe em diagrama catiônico [Al x (Fe_{total} + Ti) x Mg]. Os diagramas de variação mostram enriquecimento em SiO_2, TiO_2, FeO, Na_2O, K_2O e P_2O_5 e empobrecimento em Al_2O_3, MgO e CaO dos basaltos até os pegmatitos. Razões La/Lu_N variam entre 5,4 a 6,5 nos basaltos e 6,3 a 7,9 nos pegmatitos, mostrando que as segregações pegmatíticas são geoquimicamente evoluídas em relação às suas rochas hospedeiras. Os cristais de plagioclásio nos pegmatitos são mais sódicos que aqueles encontrados nos basaltos hospedeiros; teores de CaO dos piroxênios nos basaltos são maiores quando comparados àqueles dos pegmatitos. Os resultados da modelagem geoquímica de elementos traço mostram que é possível que ocorra o fracionamento dos pegmatitos básicos a partir de basaltos com assembleia mineral composta por: 55 % em peso de plagioclásio, 35 % em peso de clinopiroxênio, 10,0 % em peso de óxidos de ferro e titânio. O processo ocorre como cristalização fracionada com 50% de fusão residual.

Palavras-chave: Província Ígnea do Paraná; Derrames basálticos; Litogeoquímica; Cristalização fracionada; Elementos traço.

INTRODUCTION

Over the last three decades, the Paraná Igneous Province (PIP) has been the central focus of numerous geochemical, geochronological, and/or isotopic characterizations (Piccirillo and Melfi, 1988; Peate et al., 1992; Marques and Ernesto, 2004; Licht, 2018). Recent studies have sought to clarify the chemical classification, architectural framework, morphology of the basaltic flows and their relationship with volcaniclastic, volcanogenic, and sedimentary deposits interspersed with them (Arioli and Licht, 2006; Waichel et al., 2006; Rossetti et al., 2014; Licht and Arioli, 2018).

The PIP has more than 40 recorded occurrences of basic pegmatites hosted in basaltic flows (Szubert et al., 1979; Licht and Arioli, 2000; Wildner et al., 2006; Licht and Arioli, 2018; Oliveira et al., 2020), described in the state of Paraná. Magmatic segregation processes are responsible for the formation of a variety of structures within basaltic rocks, which can be present in both flows and intrusions (Hartley and Thordarson, 2009). Typical features related to magmatic segregation are spherical vesicles, vertical vesicle pipes, and differentiated pegmatitic or horizontal vesicle sheets (Philpotts et al., 1996; Merle et al., 2005; Hartley and Thordarson, 2009). For the magmatic segregation process to take place, a degree of magma crystallization around 35% is estimated to be necessary (Philpotts et al., 1996; Merle et al., 2005). At this stage, a crystalline framework is formed in magma or lava that is strong enough to allow the extraction of interstitial liquid without the mobilization of crystalline phases (Philpotts et al., 1996; Merle et al., 2005; Hartley and Thordarson, 2009).

By studying the processes that govern the crystallization of pegmatitic structures formed in basaltic lavas, it is possible to understand how these structures are generated and to comprehend the evolution of inflated pahoehoe flows from a chemical perspective. The pegmatites that are the subject of study of this work were sampled by borehole cores obtained at the Itaipu Hydroelectric Power Plant. The study area is in the city of Foz do Iguaçu, in the western portion of the state of Paraná, which is approximately 650 kilometers from the state capital, Curitiba (Figure 1). The Itaipu Hydroelectric Power Plant (Itaipu Dam), the largest of its kind in the Americas, was built on the border between Brazil and Paraguay, on top of basaltic flows from the PIP.

MATERIALS AND METHODS

The analyzed samples belong to core sections of two boreholes from the Itaipu Dam collection. Petrographic thin sections were described from the host basalt and from the basic pegmatites. Description and textural interpretations were carried out in transmitted light with a Zeiss petrographic optical microscope, in the microscopy laboratory of the Geology Department (LAPEM-UFPR) and in the Mineral and Rock Analysis Laboratory (*Laboratório de Análise de Minerais e Rochas* — iLAMIR); the software AxioVision — Zeiss was used for imaging. Textural and mineralogical aspects were observed, such as mineral assemblages, crystal interfaces, crystal sizes, and modal percentage of mineral species, in order to investigate the crystallization processes of the studied rocks.

Geochemical data used in this work were obtained in the mass spectrometer with inductively coupled plasma (ICP-MS) laboratory at the *Instituto de Geociências da Universidade de São Paulo* (IGc-USP), and at AcmeLabs (Acme Analytical Labs Ltd). Major oxides were analyzed by X-ray fluorescence (glass beads and lithium tetraborate). Trace and rare earth elements (REE) were analyzed in an ICP-MS (acid digestion of 0.2 g of sample). Unanalyzed elements are identified as non-determined (n.d.) in samples of both pegmatites and host basalts. The analytical conditions for data acquisition as well as detailed methodology are described in Costa (2015) and Titon (2016).

Mineral chemistry analyses were carried out using a Cameca SX50 electronic microprobe (equipped with 4 wavelength dispersive spectrometer (WDS) and one energy dispersive spectrometer (EDS)) in the Microanalysis Laboratory of the Institute of Geosciences and Georesources (*Istituto di Geoscienze e Georisorse* — IGG) of the National Research Council (*Consiglio Nazionale delle Ricerche* — CNR)*,* Padova, Italy. Analytical conditions for data acquisiton were as follows: 15kV for chemical determination with a current of 15 nA for plagioclase crystals and 20 nA for clinopyroxenes and oxides and a beam diameter of 1 μm. Samples were previously carbon coated. Natural and synthetic standards were used for calibration. Uncertainties are less than 1% and less than 5% for major and minor elements, respectively.

Interpretation of the analytical data and construction of geochemical diagrams were carried out using the GeoChemical Data Tool-Kit (GCDkit) software. Fe_2O_{3tot} was separated using the ratios defined according to the diagram Total Alkali - Silica (TAS - $[(Na_2O+K_2O)$ x $SiO_2]$) by Middlemost (1989): FeO/Fe_2O_3 of 0.2 and 0.3 for basalts and pegmatites, respectively. Trace element geochemical modeling was performed using fractionation equations by Cox et al. (1979), considering the host basalts as primitive rocks and the basic pegmatites as evolved rocks. Calculations were carried out based on a mineral assemblage composed by plagioclase, pyroxene, and oxides (Fe and Ti). The compositions used were those of samples L34-b2 (host basalt) and L24-a2 (pegmatite) (Table 1), on a hydrated basis. The partition coefficients used in the calculations were based on Arth (1976), for basaltic magmas (Supplementary Material 1). Normalization factors used in the C/O ratios (calculated value/observed value) followed Wood et al. (1979) for the primordial mantle.
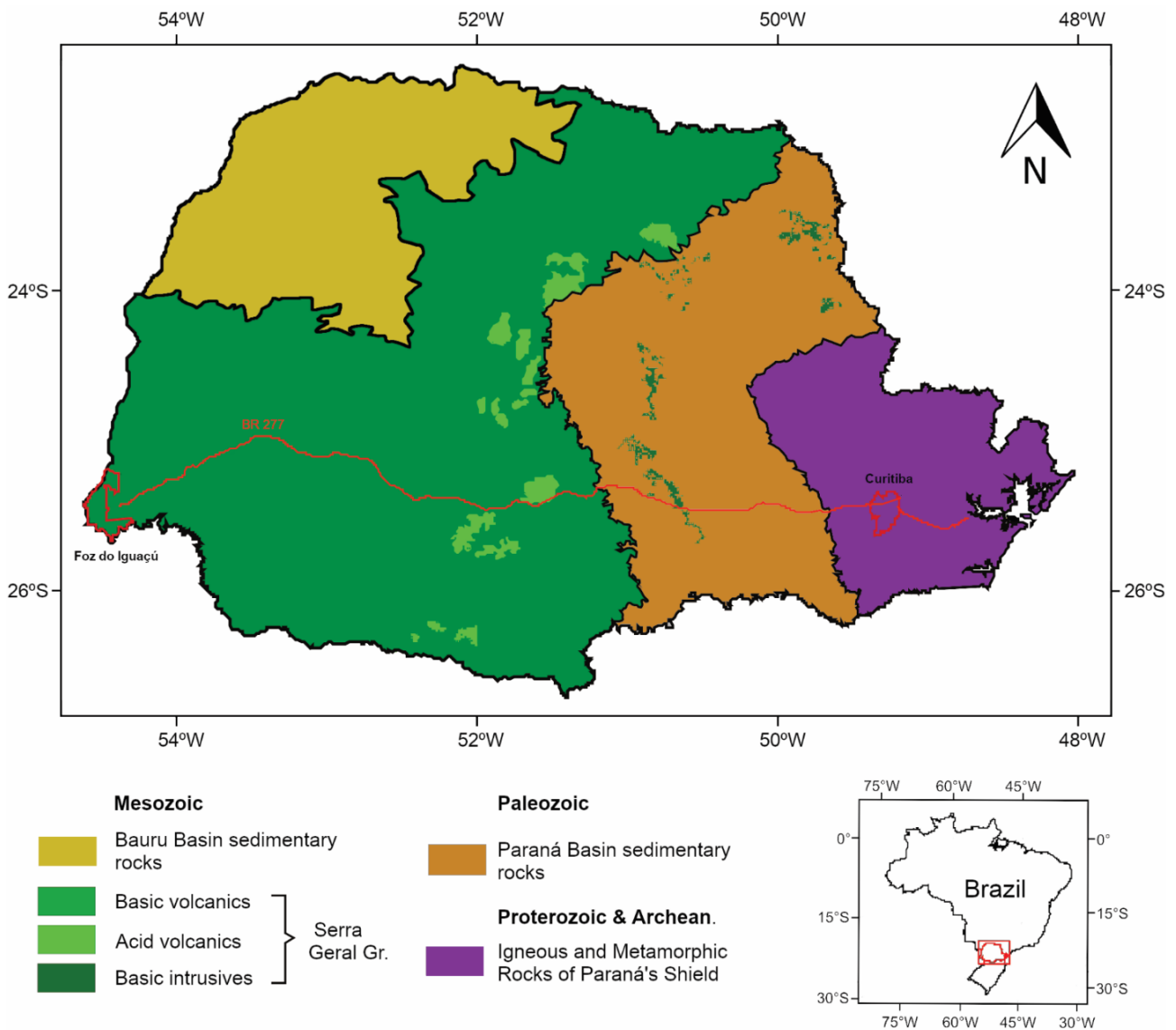
Figure 1. Map of Paraná showing Foz do Iguaçu in the westernmost portion of the state and the location of Itaipu Hydroelectric Power Plant, *ca.* 650 km from the state capital, Curitiba.

GEOLOGICAL CONTEXT

The Paraná Igneous Province

During the Early Cretaceous, the South and Southeast regions of Brazil experienced a massive magmatic event that preceded the opening of the South Atlantic Ocean, resulting in one of the largest continental basaltic provinces in the world (Marques and Ernesto, 2004; Janasi et al., 2011). The rocks of the PIP are mainly represented by basaltic flows and, subordinately, by acid volcanic rocks, characterizing a bimodal-type volcanism, in which intermediate volcanics are restricted (Marques and Ernesto, 2004; Licht,

2018). PIP basaltic magmatism is mainly composed of inflated pahoehoe-type flows formed by continuous lava injection, resulting in a process of basaltic flow inflation (Self et al., 1998).

One of the earliest descriptions of basic pegmatites in basaltic flows from the Serra Geral Group (Paraná Igneous Province — PIP) was given by Szubert et al. (1979) (*Projeto Cobre* in Itapiranga, Santa Catarina). Later, Vasconcellos et al. (2001) described the basic pegmatites as pegmatoid gabbros as part of characterization studies of Serra Geral Group basaltic flows. Basic pegmatites are observed within inflated *pahoehoe* flows in the Guarapuava region, in which top and bottom breccias also occur (Arioli et al., 2008).

In Salto do Lontra (Paraná), Ferreira (2011) describes magnetically susceptible basic pegmatites inside a 50-meter-thick inflated pahoehoe flow. More recently, working in the southwestern portion of Paraná, Oliveira et al. (2020) systematically describe the occurrence of pegmatite segregations in multiple geochemically distinguished basaltic flows, divided according to the classification proposed by Licht (2018).

The rocks that make up the PIP have a bimodal characteristic (Piccirillo and Melfi, 1988; Licht, 2018), approximately 90% of the rocks are mafic, classified as basalts and andesi-basalts, and the remaining 10% are felsic, classified

Table 1. Chemical composition of host basalts and basic pegmatites from Itaipu Dam, western Paraná. Total Fe is expressed as FeO.

	Sample	L24-a1	L24-a2	L24-k1	L24-k2	L34-b1	L34-b2	L118-b1	L118-b2
	Lithology	Basalt	Pegmatite	Pegmatite	Basalt	Pegmatite	Basalt	Basalt	Pegmatite
Major oxides (wt. %)	SiO_2	49.8	52.9	49.0	52.4	51.7	49.8	49.4	50.1
	TiO_2	2.45	2.48	2.56	2.73	2.83	2.28	2.27	2.98
	Al_2O_3	12.7	11.6	12.7	11.9	11.7	12.9	13.0	11.8
	FeO	15.1	15.9	14.7	15.1	15.9	14.8	12.9	16.9
	MnO	0.23	0.20	0.18	0.16	0.21	0.20	0.21	0.22
	MgO	4.77	3.24	5.59	3.82	3.51	5.53	5.46	4.10
	CaO	9.78	6.76	9.74	6.31	6.55	9.41	9.58	7.76
	Na_2O	2.47	2.67	2.52	2.83	3.49	2.47	2.41	2.47
	K_2O	1.04	1.83	1.10	1.93	1.76	1.01	0.99	1.42
	P_2O_5	0.27	0.48	0.37	0.65	0.49	0.24	0.24	0.31
	LOI	0.60	0.80	0.64	0.87	1.40	0.90	1.10	1.60
	Sum	99.3	98.9	99.2	98.7	99.7	99.7	99.6	99.6
CIPW (%)	qz	3.59	9.48	1.61	8.11	4.41	2.71	2.58	5.93
	pl	42.5	38.1	42.7	39.5	42.0	43.1	43.2	39.1
	or	6.32	11.2	6.68	11.8	10.7	6.15	6.03	8.69
	di	22.3	14.1	21.8	11.2	15.7	20.2	20.7	17.1
	hyp	15.3	16.4	17.0	18.0	15.7	18.3	18.1	17.6
	ilm	4.77	4.86	4.99	5.36	5.55	4.44	4.43	5.85
	mag	4.51	4.77	4.38	4.54	4.77	4.44	4.47	5.07
	ap	0.65	1.16	0.88	1.55	1.18	0.58	0.58	0.74
	mg#	0.25	0.18	0.21	0.29	0.19	0.28	0.28	0.21
Trace elements (ppm)	Ba	322	556	333	571	438	314	313	440
	Rb	21.7	41.8	25.2	48.0	41.6	20.4	20.6	30.2
	Sr	365	343	363	373	334	367	378	351
	Zr	155	281	164	303	267	156	149	218
	Nb	13.9	28.8	16.9	42.9	24.1	13.1	13.1	18.4
	Ni	n.d.	n.d.	n.d.	n.d.	7.80	24.9	26.4	11.7
	Co	n.d.	n.d.	n.d.	n.d.	35.8	43.2	45.8	38.6
	Zn	101	101	109	126	94.0	63.0	68.0	93.0
	Cr	n.d.	n.d.	n.d.	n.d.	30.0	150	130	20.0
	Y	29.9	44.1	31.0	44.9	42.7	26.0	27.4	34.4
	Ta	n.d.	n.d.	n.d.	n.d.	1.50	0.80	0.90	1.10
	Hf	3.90	7.30	4.20	7.80	6.70	4.30	4.20	6.10
	Ga	n.d.	n.d.	n.d.	n.d.	21.3	17.7	19.1	18.9
	Th	2.50	4.80	2.50	5.10	5.30	2.60	2.40	3.80
	U	0.50	0.90	0.50	1.00	0.90	0.40	0.50	0.80
	V	n.d.	n.d.	n.d.	n.d.	498	485	493	556
	Mo	n.d.	n.d.	n.d.	n.d.	0.40	0.30	0.40	0.70
	Cu	n.d.	n.d.	n.d.	n.d.	341	206	324	312
	Pb	3.60	6.50	3.70	6.20	2.30	0.70	0.80	0.80

Table 1. Continuation.

	Sample	L24-a1	L24-a2	L24-k1	L24-k2	L34-b1	L34-b2	L118-b1	L118-b2
	Lithology	Basalt	Pegmatite	Pegmatite	Basalt	Pegmatite	Basalt	Basalt	Pegmatite
	La	22.1	39.7	24.6	44.9	39.4	22.1	20.5	30.0
	Ce	47.4	85.5	53.3	94.6	85.7	46.2	44.1	62.7
	Pr	6.30	10.7	7.30	12.1	10.4	5.90	5.70	7.60
	Nd	24.8	42.7	27.6	48.5	43.1	24.6	25.5	30.3
	Sm	5.90	9.70	6.60	10.6	8.90	5.30	5.40	6.50
	Eu	1.90	2.90	2.10	3.20	2.50	1.80	1.80	2.00
	Gd	5.40	8.80	6.10	9.70	9.40	5.40	5.60	7.20
REE	Tb	0.90	1.40	1.00	1.50	1.40	0.90	0.90	1.20
(ppm)	Dy	5.20	8.30	5.70	8.80	8.00	5.20	5.20	6.60
	Ho	1.20	1.80	1.20	1.80	1.60	1.10	1.10	1.30
	Er	2.90	4.50	3.00	4.60	4.80	3.00	2.90	3.50
	Tm	0.40	0.70	0.50	0.70	0.70	0.40	0.40	0.50
	Yb	2.60	4.10	2.60	4.20	4.40	2.50	2.70	3.60
	Lu	0.40	0.60	0.40	0.60	0.60	0.40	0.40	0.50
	SumETR	128	221	142	246	221	125	122	164
	La_N/Lu_N	5.80	6.90	7.90	6.50	6.90	5.80	5.40	6.30
	Licht (2018)	Type 1 S	Type 2	Type 2	Type 1 S	Type 4	Type 1 S	Type 1 S	Type 3

LOI: Loss on ignition; S: South; n.d.: non-determined.

mainly as rhyolites and rhyodacites (Marques and Ernesto, 2004). The PIP has been the subject of numerous geochemical studies (Bellieni et al., 1984; Piccirillo and Melfi, 1988; Peate et al., 1992; Gomes et al., 2018; Licht, 2018) seeking to understand the evolution of its basaltic flows. Bellieni et al. (1984) and Mantovani et al. (1985) proposed to divide the PIP into distinct compartments, mainly using the content of TiO_2. The low TiO_2 tholeiitic suite, in the northern regions (Low titanium basalts: 1.4 ± 0.1 wt.% TiO_2; 0.04 wt.% P_2O_5; < 300 ppm Sr; < 30 ppm La; < 60 ppm Ce; < 500 ppm Ba; $^{87}Sr/^{86}Sr$ 0.707 – 0.710) and the high TiO_2 tholeiitic suite in the southern regions (High titanium basalts: 3.4 ± 0.1 wt.% TiO_2; $^{87}Sr/^{86}Sr$ 0.704 – 0.706 and high levels in Rb, Th, and U). Subsequently, using SiO_2 content, trace elements and incompatible elements concentrations such as Sr, Zr and Y, Peate et al. (1992) and Peate (1997) further subdivided the PIP into six distinct units or "magmatypes". The high TiO_2 basalts (HTiB) were divided into 3 types, called *Urubici*, *Pitanga*, and *Paranapanema*, while the low TiO_2 basalts (LTiB) were divided into *Gramado*, *Esmeralda*, and *Ribeira*.

Using a database of more than 5,600 chemical analyses of outcrops and borehole samples, Licht (2018) proposes a new statistical division of basaltic flows from the PIP. Statistical analysis of the geochemical data revealed gaps of SiO_2 (62.02 wt.%), Ti (2.8499 wt.%), Zr (522.15 ppm), and P (0.4127 wt.%), which result in high level (H) and low level (L) groups that allow the subdivision of PIP volcanics into 16 different groups. Basic rocks (SiO_2 < 62.02 wt.%) form 8 groups and acid rocks (SiO_2 > 62.02 wt.%) another

8 groups. According to this new division, the most abundant rocks in the PIP are classified into types 1 (LSi, LZr, LTi, LP) and 4 (LSi, LZr, HTi, HP). Additionally, type 1 rocks are subdivided according to geographical criteria and stratigraphic position into Type 1 Center-North and Type 1 South (Licht, 2018).

In the 1970s, during the construction of the Itaipu Dam, numerous boreholes were drilled, which allowed the study and more detailed characterization of the province's stratigraphy in the region. Costa et al. (2014) separated basalts from the Itaipu Dam region into 10 different morphological units based on geochemical analyses and facies description of core samples. Geochemical and textural characteristics adopted for this division reflect different processes during the eruption episodes that generated these units. Overall, the PIP lava sequence in the Itaipu region is composed of two interspersed types of high TiO_2 magmas that occur as flows with varied morphologies (pahoehoe, rubbly pahoehoe and a'a'), which were conditioned by different effusion rates (Costa et al., 2014).

Basic pegmatites

Pegmatites are very coarse-grained rocks, usually related to late crystallization of acid magmas. This term is used in two different senses: sometimes to designate the textural aspect, sometimes to name a unit of rock. Jahns (1955) defined pegmatites as: "holocrystalline rocks that possess, at least in part, a very coarse fabric, having as major mineral constituents those typically found in igneous rocks, but with

Geol. USP, Sér. cient., São Paulo, v. 23, n. 4, p. 65-85, Dezembro 2023

- 69 -

the characteristic of presenting extreme textural variations, especially with regard to the size of the crystals".

Pegmatitic features are also described in the literature associated with basaltic flows and, more restrictively, with plutonic bodies of mafic composition (Walker, 1953; Puffer and Horter, 1993; Hartley and Thordarson, 2009; Oliveira et al., 2020). Basic pegmatites are somewhat frequent in pahoehoe-type lava flows that have undergone inflation, which increases their thickness and extent, as defined by Self et al. (1998). Inflation occurs as the top and bottom portions of the flow are transformed into rigid crusts by rapid cooling (quenching), while the core remains thermally isolated and liquid and rich in upward migrating volatile bubbles. High temperatures in the flowing core are maintained by the continuous injection of lava (Figure 2). After lava injections cease, inflation is terminated and the temperature inside the system decreases and, as a result, processes that lead to the

concentration of differentiated liquids occur — which are genetically associated with the host rock. Consequently, vertical bodies (cylinders) are formed resulting from bubble coalescence; when they encounter an upper rigid barrier, they become horizontal (sheets), classified as basic pegmatites (Figure 2). Therefore, the main characteristics of these pegmatitic segregations are: coarser granulation than the host rock, abrupt contact between the pegmatites and the host rock and mineral assemblage similar to that of basalts. Although composed of the same minerals, pegmatites are geochemically more evolved and occur in thick basaltic flows or, less commonly, in intrusions (Walker, 1953).

Pegmatites have remarkably contrasting textures and structures. Greenough and Dostal (1992) describe coarse-grained pegmatitic layers made up of pyroxene, plagioclase, subordinate skeletal Fe-Ti oxides and a quartz-feldspathic matrix forming sharp contacts with the surrounding host
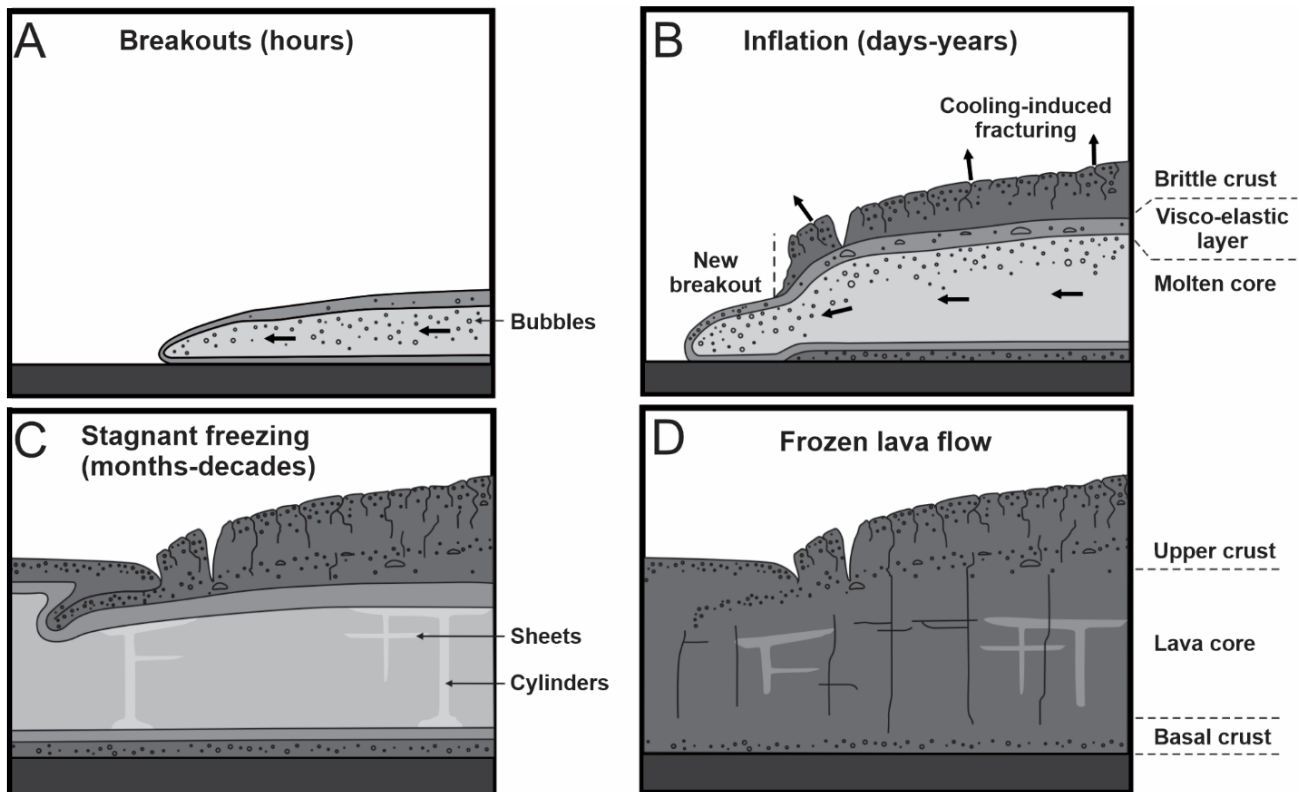
Source: adapted from Self et al. (1997).

Figure 2. Schematic cross section of emplacement of a generic inflating *pahoehoe* sheet flow. Vertical scale is 5-50 meters. (A) Flow starts as a small, slow-moving, lobe of molten lava held inside a stretchable, chilled viscoelastic skin with brittle crust on top. Bubbles are initially trapped in both the upper and basal crusts. (B) Continued injection of lava into the lobe results in inflation (lifting of the upper crust) and new breakouts. During inflation, bubbles rising from the fluid core become trapped in the viscoelastic mush at the base of the upper crust, forming horizontal vesicular zones. The growth of the lower crust, in which pipe vesicles develop, is much slower. Relatively rapid cooling and motion during inflation results in irregular jointing in the upper crust. (C) After stagnation, diapirs of vesicular residuum form vertical cylinders and horizontal sheets within the crystallizing lava core. Slow cooling of the stationary liquid core forms more regular joints. (D) Emplacement history of flow is preserved in vesicle distribution and jointing pattern of frozen lava.

basalt. The layers show intersertal texture in a matrix of devitrified glass. Within basalt flows from the Columbia River Group (USA), pegmatitic segregations occur with diktytaxitic texture and containing up to 15% inter-crystalline voids. The mineral assemblage is comprised of plagioclase, clinopyroxene, olivine, and opaque minerals all encompassed by a glassy mesostasis (Hartley and Thordarson, 2009). Although pegmatites have a coarser grainsize than their host lava, they are largely aphyric. Pyroxene crystals within the segregations often show a more well-developed ophitic texture than those of the host lava and they may display skeletal textures or graphic intergrowth textures (Walker, 1953; Puffer and Horter, 1993; Philpotts et al., 1996). The occurrences of basic pegmatites in the PIP are similar to those described elsewhere. They present a sharp contact with the host basalt and, mineralogically, both lithotypes are very similar. The most distinguishing feature is that crystals can be 5 to 20 times larger in pegmatites than host basalts, reaching up to 60 mm in length (Oliveira et al., 2020). In the southwestern region of the state of Paraná, two occurrences of pegmatites are described by Soares (2016). They are medium- to coarse-grained porphyritic in a fine to very fine brownish to reddish matrix. Submillimetric microvesicles and, less frequently, centimeter-sized vesicles filled with clay minerals and celadonite are common.

The definition for pegmatitic segregations has been modified in the literature as new studies have been carried out. The terms seek to reflect processes of formation along with textural and compositional aspects. Several terms have been used in the past to refer to basic pegmatites. Among the most widely used are: pegmatitoids (an obsolete term used by Lacroix, 1929; Dunham, 1933; Santin, 1969); differentiated pegmatites by Walker (1953); mafic pegmatites by Greenough and Dostal (1992) and Kontak et al. (2002); pegmatitic segregations by Puffer and Horter (1993); pegmatoidal gabbro-dolerite by Jefferson et al. (1994); pegmatitic magmatic segregations by Philpotts et al. (1996); gabbros by Vasconcellos et al. (2001); pegmatoid gabbros by Arioli (2008); and basic pegmatites by Oliveira et al. (2020) and Titon et al. (2021).

Of the more than 40 recorded occurrences of basic pegmatites in the PIP, around 16 occurrences of basic pegmatites are described in southwestern Paraná by Licht (2001) and Oliveira et al. (2020), and yet another 14 occurrences described by Arioli and Licht (2006). In the Guarapuava region, 8 new occurrences are also described in the literature (Arioli et al., 2008). Basic pegmatites are identified and described in only 2 of the basaltic flow units previously studied in the Itaipu Dam region. They are named units 5 and 10, according to the nomenclature given by Costa et al. (2015). Unit 5 has a maximum thickness of 49 meters and is composed of massive aphanitic basalt with a vesicular/amygdaloidal upper portion. The sub-horizontal pegmatitic

segregations are in the intermediate portion of the flow and have interspersed contact with the host basalt and a medium equigranular phaneritic texture. Unit 10 has a maximum thickness of 40 meters and is composed of aphanitic basalt with massive core and less pronounced vesicular/amygdaloidal upper portion. Pegmatites of 5 to 50 centimeters thick are described, with textural characteristics like those found in unit 5 (Costa et al., 2015).

RESULTS

Petrographic aspects of host basalts and pegmatites

Basalts display a microporphyritic texture in a fine, equigranular, and phaneritic matrix. They are holocrystalline to hypocrystalline, intergranular to subophytic or interstitial, (due to the restricted occurrence of devitrified interstitial glass in the matrix) and massive. They are essentially composed of 50 wt.% labradorite, 30 to 35 wt.% augite, and 5 to 10 wt.% metallic oxides, chemically identified as magnetite and Ti-magnetite. Subordinately, the occurrence of iron hydroxides gives the matrix a reddish color; clay minerals appear as filling diktytaxitic cavities or resulting from devitrification processes (up to 5 wt.%). Labradorite occurs as fine-grained compositionally zoned microphenocrysts (up to 1.2 mm) and as very fine-grained crystals in the matrix (0.2 – 0.5 mm) with subhedral habit (Figure 3A). Crystals are sericitized and fractured with fine plagioclase aggregate crystals displaying bifurcated end features (also observed in pegmatite plagioclase crystals). This textural feature, known as swallow-tail, frequently noticed in small-sized plagioclase phenocrysts, is characterized by hollow, H-shaped crystal margins (Renjith, 2014). It is interpreted as a suddenly quenched skeletal texture associated to a rapidly increased growth rate in the final crystallization stages, dependent on a high degree of undercooling (Shelley, 1992; Viccaro et al., 2010). Augite is found in the matrix and as microphenocrysts with anhedral granular habit (Figure 3A). It is fine to very fine-grained with a grain size up to 0.8 mm and is locally altered to opaque minerals (Figures 3B and 3C). Metallic oxides occur as very fine to fine-grained microphenocrysts (up to 2.0 mm). They display anhedral habit and irregular boundaries, with elongated or tabular shape; skeletal and poikilitic textures are common, with plagioclase and clinopyroxene inclusions. Opaque crystals in the matrix are associated with iron hydroxides and augite alteration products. Restricted interstitial glass is intensely oxidized and reddish to orange in color (Figure 3C). It forms very fine aggregates (between 0.1 to 0.4 mm) associated with secondary minerals originated from devitrification processes. This secondary material represents up to 5 wt.% of the rock,

Geol. USP, Sér. cient., São Paulo, v. 23, n. 4, p. 65-85, Dezembro 2023

- 71 -
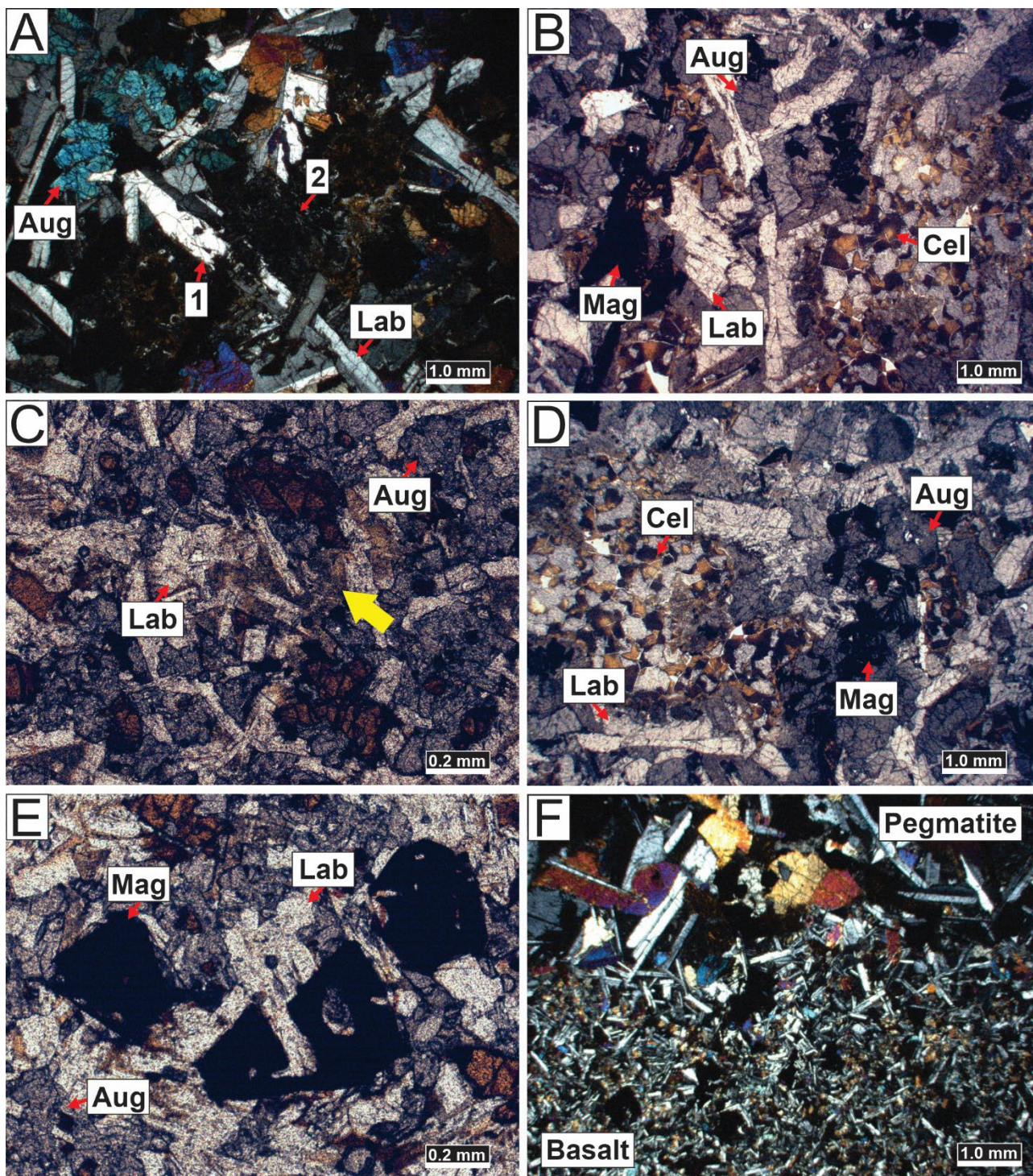
Aug: augite; Cel: celadonite; Lab: labradorite; Opq: metallic oxides (opaques); PPL: plane polarized light; XPL: cross polarized light.

Figure 3. Photomicrographic images of samples studied. (A) Different crystallization phases of labradorite in host basalts: 1- microphenocrystals; 2- fibrous and needle-like crystals in the matrix (L24-a in XPL). (B) Skeletal texture in metallic oxides in host basalt. Note diktytaxitic cavities filled by celadonite (L24-k2 in PPL). (C) Diktytaxitic cavities filled by clay minerals (yellow arrow) and augite crystals altered to metallic oxides (L24-k2 in PPL). (D) Medium-grained, equigranular and phaneritic basic pegmatite. Skeletal texture in metallic oxides and microvesicles filled by celadonite are present (L24-k1 in PPL). (E) Metallic oxide crystals encompassing labradorite crystals in basic pegmatite matrix (L24-k1 in PPL). (F) Interface between host basalt and basic pegmatite are abrupt with no discernible transition (L24-a in XPL).

mainly occurring in the interstices between crystals in the matrix. Diktytaxitic cavities correspond to about 2 wt.% of the rock; they have very irregular shapes and boundaries and are filled with clay minerals and celadonite; sizes vary between 0.2 to 0.4 mm.

Pegmatites are fine- to coarse-grained, inequigranular and phaneritic, holocrystalline to hypocrystalline, and subophitic to intergranular, with variolitic structure (Supplementary Material 2). Phenocrystals reach up to 5.0 mm and crystals in the matrix range between 0.4 to 1.0 mm (Figures 3B and 3D). Pegmatites are composed of 30 wt.% labradorite, 40 wt.% augite, and up to 10 wt.% of metallic oxides (also magnetite and Ti-magnetite). Subordinately, traces of apatite occur (< 0.1 mm); up to 15 wt.% of diktytaxitic cavities and microvesicles and 5 wt.% of devitrified aggregates. Labradorite occurs as subhedral phenocrystals, ranging from 3.0 to 5.0 mm (Figure 3D); crystals are clear and without compositional zoning. Amidst the phenocrystals and associated with the microvesicles, aggregates formed exclusively by very thin acicular plagioclase occur, with an axiolitic texture. Augite occurs as phenocrystals and in the matrix, with sizes ranging from 0.8 to 4.0 mm. They are light brownish anhedral granular to subhedral crystals and associated with skeletal metallic oxides (Figures 3B and 3D). Metallic oxides display acicular and square-like shapes (Figure 3E) and are fine to coarse-grained (up to 5.0 mm). They occur as inclusions in augite and labradorite crystals, as alteration product (of augite), in the matrix an also as phenocrystals with skeletal or poikilitic texture. Diktytaxitic cavities and microvesicles are filled by clay minerals and celadonite (Figures 3B and 3D). The boundary between basalt and pegmatite is abrupt and undulating (Figure 3F), with no discerning variation in mineral assemblages. This transition is evidenced by the sudden and marked change in the grain size between the lithologies.

Lithogeochemistry

Eight samples were analyzed to determine major oxides, trace and REE, 4 of which were from pegmatites and 4 from host basalts. Table 1 contains major oxide data and Lost on Ignition (LOI) in weight percentage as well as values and trace and REE data expressed in ppm.

Major oxides

All four pegmatite samples are supersaturated in SiO_2, with normative quartz varying between 1.6 wt.% (L24-k1) and 9.5 wt.% (L24-a2). Other normative minerals are plagioclase (38.1 to 43.2 wt.%), orthoclase (6.0 to 11.8 wt.%), diopside (11.2 to 22.3 wt.%), hypersthene (15.4 to 18.3 wt.%), ilmenite (4.4 to 5.9 wt.%), magnetite (4.4 to 5.1 wt.%) and apatite (0.6 to 1.6 wt.%). The magnesium number (Mg/ (Mg+Fe^{2+})

ranges between 0.18 to 0.22 in pegmatites and 0.26 to 0.28 in basalts. TiO_2 content varies between 2.48 to 2.98 wt.% in pegmatites and 2.27 to 2.73 wt.% in basalts (Table 1). There is a direct correlation between the evolutionary degree of the rocks and the aforementioned chemical contents, in which basalts have generally lower TiO_2 values than pegmatites and the opposite occurs with the magnesium number (mg#). This indicates a slightly more evolved character of pegmatites in relation to basalts.

In the TAS diagram, of Le Maitre et al. (2002), host rocks are classified as basalts and pegmatitic segregations are classified as basalt, andesi-basalts, and basaltic trachy-andesite, showcasing an enrichment of silica and alkalis from host rocks to pegmatites (Figure 4). High K_2O contents, evidenced by the occurrence of normative orthoclase, reflect the presence of celadonite in microvesicles and diktytaxitic cavities. In the AFM diagram [A = (Na_2O+K_2O); F = $(FeO+Fe_2O_3)$; M = (MgO)], by Irvine and Baragar (1971), the samples are concentrated in the field of the tholeiitic series (Figure 5A), with host basalts having higher MgO contents, and pegmatites grouped closer to the vertex that represents the sum of alkalis. The higher evolutionary degree of pegmatites when compared to basalts is further marked by this trend. In the cation diagram, by Jensen and Pyke (1983), samples are classified as high-Fe tholeiitic basalts, consistent with its continental character (Figure 5B). Pegmatites are more enriched in Fe_{tot} + Ti and host basalts present higher levels of MgO, which indicates the more primitive character of these rocks.

Geochemical variation diagrams (Figure 6), show an enrichment of SiO_2 and TiO_2 and mild enrichment of FeO, Na_2O, and P_2O_5, from basalts to pegmatites. Conversely, there is a depletion in Al_2O_3, MgO, and CaO in pegmatites when compared to basalts. Depletion in Al_2O_3, MgO, and CaO is probably related to crystal fractionation of augite and labradorite from basalts in relation to pegmatites (Cox et al., 1979; Oliveira et al., 2020). The decrease in TiO_2 contents in both basalts and pegmatites is linked with the crystallization of ilmenite and Ti-magnetite along with FeO, which, in turn, can also be incorporated in augite. Pegmatites have higher SiO_2 contents and, in general, are richer in TiO_2 when compared to basalts. Depletion in Al_2O_3, along with the consumption of CaO in basalts reflects more calcic plagioclase members and higher Na_2O contents in pegmatites reflect more sodic plagioclase members which, again, attests for the higher degree of differentiation for pegmatites.

Trace and rare Earth elements

Zirconium is an important petrogenetic element due to its incompatible character in basic magmas (Rollinson and Pease, 2021). Therefore, during fractional crystallization processes, it tends to be concentrated in the residual melt. Thus, Zr was used as a fractioning element for trace element diagrams (Figure 7).
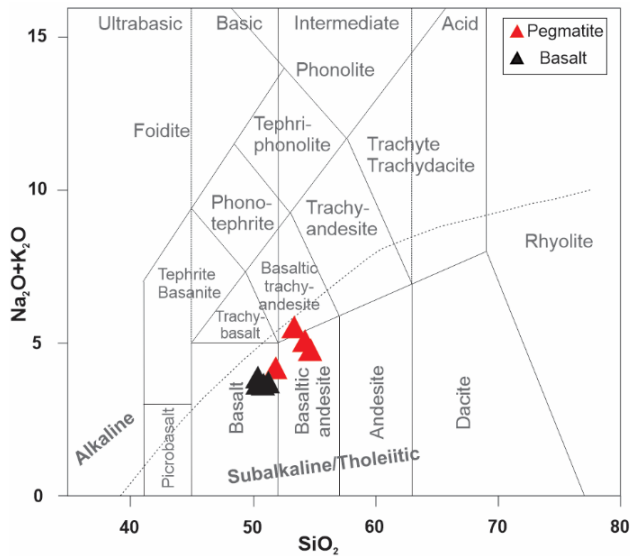
Geol. USP, Sér. cient., São Paulo, v. 23, n. 4, p. 65-85, Dezembro 2023

- 73 -

Figure 4. TAS diagram (Total alkalis *versus* silica - [(Na₂O+K₂O) x SiO₂]) from Le Maitre et al. (2002). Dotted line separates the subalkaline/tholeiitic and alkaline series, as defined by Irvine and Baragar (1971).
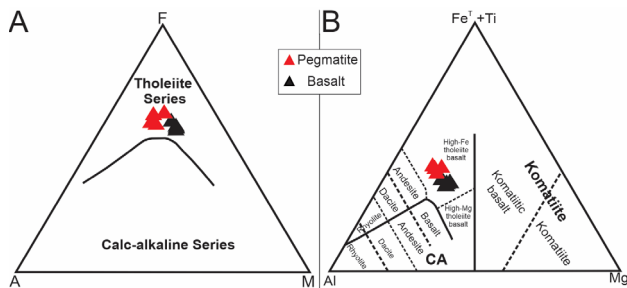

Figure 5. (A) AFM diagram [A= (Na₂O+K₂O); F= (FeO+Fe₂O₃); M= (MgO)] from Irvine and Baragar (1971). (B) Cation plot [Al x (Fe_tot+Ti) x Mg] from Jensen and Pyke (1983).

Zr contents range from 148 to 156 ppm in basalts and from 164 to 303 ppm in pegmatites (Table 1). Nickel, a compatible element during differentiation of basic magmas (Oliveira et al., 2020; Rollinson and Pease, 2021), tends to be concentrated in the host basalts, being incorporated in the first crystallization phases (*i.e.*, metallic oxides, pyroxenes). On the other hand, incompatible elements (*e.g.* large ion lithophile elements — LILE or REE), such as Rb and La, tend to concentrate in residual melts (Cox et al., 1979; Rollinson and Pease, 2021). Consequently, such elements are found in greater amount in the pegmatites, which are crystallized from late, residual liquids. Thus, when compared to host basalts, pegmatites are enriched in Rb, La, and Ce.

The trace element diagram normalized to the primordial mantle of Wood et al. (1979) indicates that pegmatites are overall enriched in trace elements when compared to host basalts (Figure 8). The negative anomaly in Sr for both rock groups suggests that plagioclase was an early fractionating mineral. The higher content of P₂O₅ in most pegmatite samples (Figure 6) reflects the incompatibility of this element during the crystallization process of mafic liquids. Scarce apatite crystals are then crystallized in the final stages of pegmatite formation, depleting P₂O₅ and other incompatible elements in the segregated liquid (*e.g.* Y and La). The low Uranium concentration indicates that the source of these rocks was mantle-derived, possibly without significant crustal contamination (Oliveira et al., 2020). There is an enrichment of LILE-type elements, such as Ba, Rb, and K in relation to high field strength elements (HFSE), such as Nb, Zr, Ti, and Y. Relative trace element concentrations for pegmatites gradually contrast those from host basalts, indicating different degrees of fractionation for the pegmatitic segregations.

REE chemical signatures show parallel patterns for all samples (Figure 9), suggesting that the two distinct groups of rocks are co-magmatic. In addition, there is enrichment in light rare earth elements (LREE) in relation to heavy rare earth elements (HREE) for both groups of rocks. Pegmatites are more differentiated in LREE than host basalts, however HREE signatures are similar for pegmatites and basalts. All samples are enriched in REE when compared to the chondrite of McDonough and Sun (1995); although host basalts REE signatures are closer to those of the chondrite, showcasing its more primitive character. La/Lu_N ratios vary between 5.4 to 6.5 in basalts and 6.3 to 7.9 in pegmatites, indicating that the latter group is more differentiated. Total amount of REE in pegmatites (∑REE) is greater than that of host basalts (Table 1). Apatite has a high partition coefficient for HREE (Prowatke and Klemme, 2006; Rollinson and Pease, 2021), therefore it is suggested that, although in minor amounts in the rock, such elements are largely concentrated in this mineral. The absence of a Europium (Eu) anomaly in pegmatites, expected in cases where the source rock has retained this element due to distinct melt rates associated with melt/solid compatibility, can be explained by the fact that the two rock lithotypes are very similar in geochemical and mineralogical terms. Both the source rock (host basalt) and the segregated phase (pegmatites) have significant amounts of plagioclase in their mineralogical compositions. Similar amounts of plagioclase in both rocks and subtle changes in plagioclase composition (bytownite to labradorite) would not be expressive enough to characterize a negative anomaly of Eu in pegmatites. The observed geochemical and mineralogical changes from a basalt to a basic pegmatite are of a more subtle character, therefore both systems would have similar intakes of Eu, rendering a negative Eu anomaly difficult to observe.
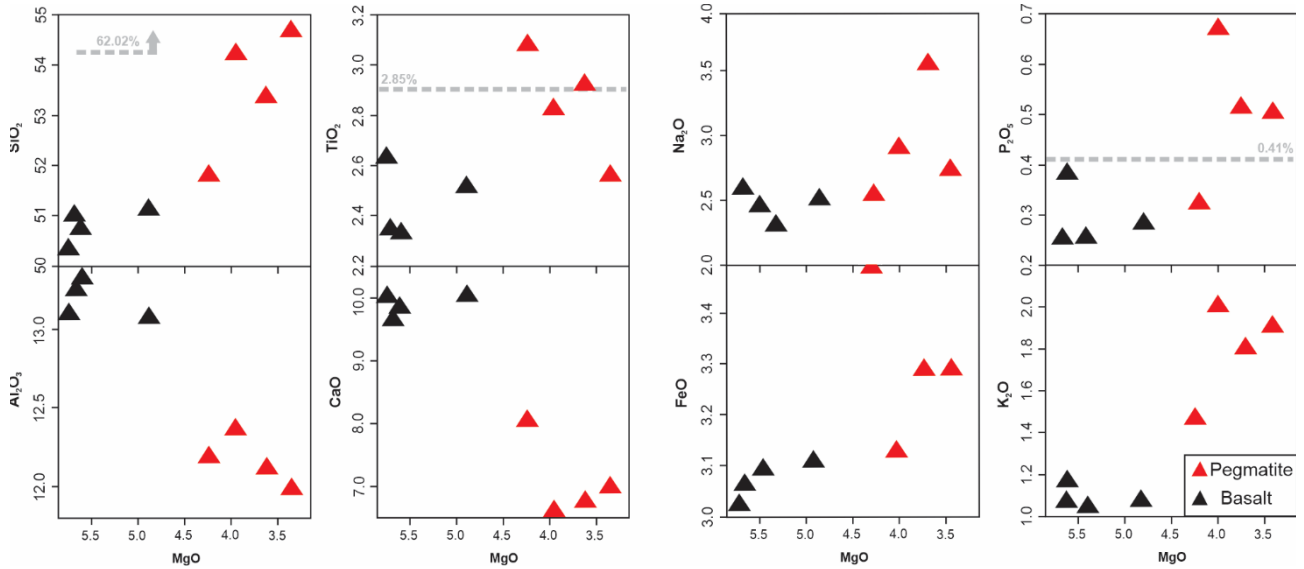
Figure 6. Fenner-type variation diagrams for major oxides for host basalts and basic pegmatites. Dotted gray lines represent the limits of elements according to the geochemical classification of Licht (2018) for the PIP, that is: LSi < 62.02% < HSi; LZr < 522 ppm < HZr; LTi < 2.85% < HTi and LP < 0.413% < HP.
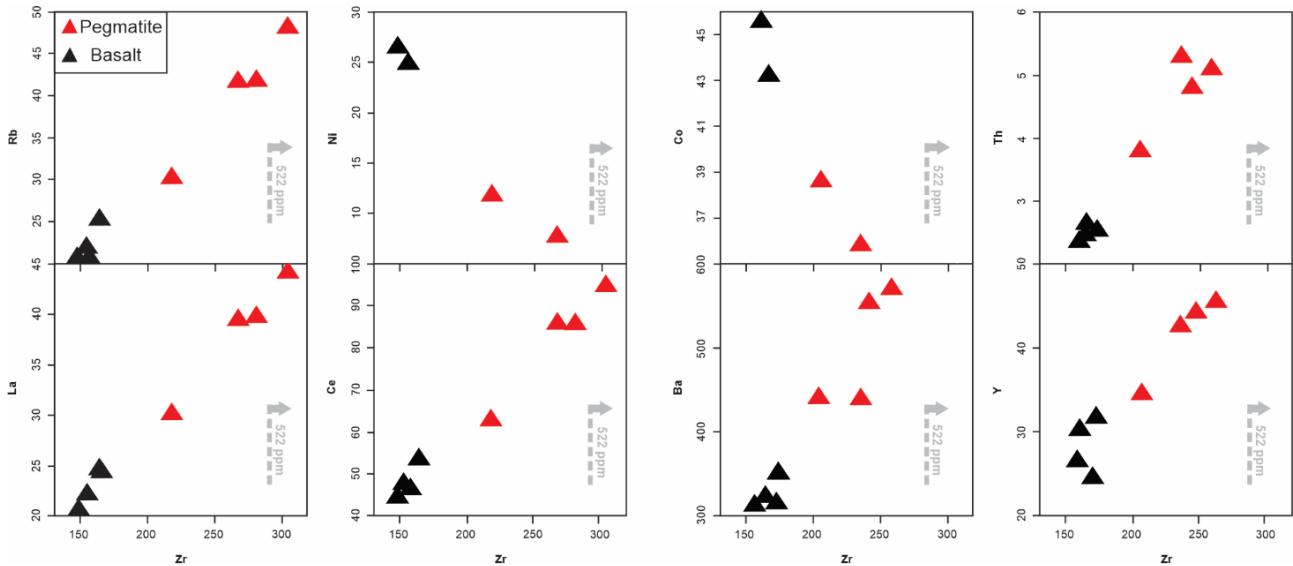

Figure 7. Variation diagrams for trace elements for host basalts and basic pegmatites. Dotted gray lines represent the limits of elements according to the geochemical classification of Licht (2018) for the PIP, that is: LSi < 62.02% < HSi; LZr < 522 ppm < HZr; LTi < 2.85% < HTi and LP < 0.413% < HP.

Mineral chemistry

Electron microprobe analyses (EMPA) were carried out on plagioclase, pyroxene, and metallic oxide crystals in four samples (Table 2): two from pegmatites and two from host basalts.

In total, ten plagioclase crystals from basalts and pegmatites were analyzed, amounting to 55 points analyzed.

The Or-Ab-An (Deer et al., 2000) diagram was used to classify the mineral species. Representative EMPA chemical analyses are shown in Table 2. Chemical compositions for all the analyzed points can be found in Supplementary Material 3, of this article. In host basalts, plagioclase chemical compositions range from labradorite to bytownite (An_{54} to An_{85}). The lowest An value (An_{54}) corresponds to the rim
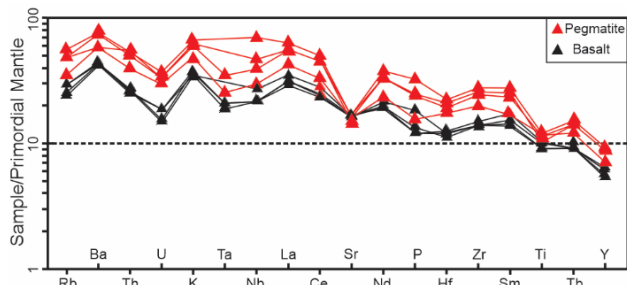
Figure 8. Trace element diagram normalized by the primordial mantle of Wood et al. (1979) for host basalts and basic pegmatites.
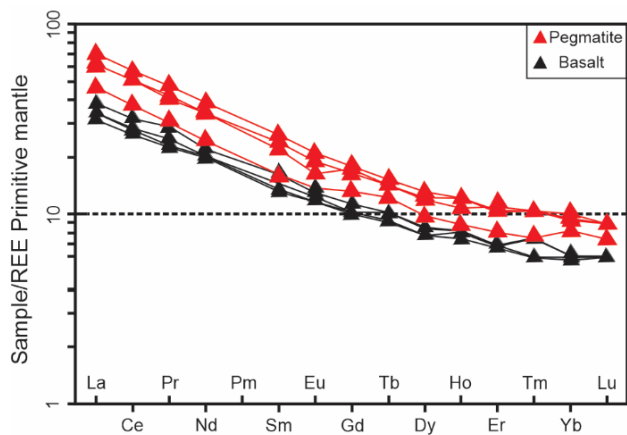

Figure 9. Rare Earth Elements diagram normalized by the chondrite of McDonough and Sun (1995) for host basalts and basic pegmatites.

of one of the plagioclase crystals. In pegmatites, plagioclase chemical compositions also vary from labradorite to bytownite (An$_{57}$ to An$_{72}$), but display a narrower range, with generally higher sodium/calcium ratios in the analyzed crystals from the pegmatites compared to the basalts (Figure 10). In general, plagioclase crystals that occur in pegmatites are more sodium-rich than those in host basalts.

A total of nine clinopyroxene crystals were analyzed, six of them from the host basalts and 3 from pegmatites, amounting to a total of 47 analyzed points. The Wo-En-Fs (Morimoto, 1988) diagram was used to classify the mineral species. Representative EMPA chemical analyses are shown in Table 2 and full chemical compositions for all the points analyzed can be found in Supplementary Material 3 of this article. Almost all clinopyroxene crystals are classified as augite, apart from rare pigeonite crystals in the matrix of host basalt L24-a1 (Figure 11). Wollastonite (Wo) content in host basalts ranges from 36.4 to 44.0% in augite and 10.0 to 10.3% in pigeonite. In pegmatites, these contents are lower, ranging from 34.6 to 42.2% and clinopyroxene crystals are exclusively classified as augite. With respect to the silica

content, the composition of augite crystals is very similar: 48.7 to 51.2 wt.% in host basalts and 49.3 to 51.2 wt.% in pegmatites (Supplementary Material 3).

MgO contents are also similar, ranging from 11.1 to 16.9 wt.% in host basalts and 13.5 to 15.0 wt.% in pegmatites, however, magnesium contents are less dispersed in the latter group. Calcium content is comparable for both groups of rocks: 16.8 to 19.7 wt.% in host basalts and 15.5 to 18.9 wt.% in pegmatites, but with a slight depletion of calcium in pegmatites.

Overall, clinopyroxene and plagioclase crystals found in host basalts are richer in CaO. In pegmatites, clinopyroxene is more enriched in FeO (12.3 to 14.4 wt.%); MgO contents are similar for both groups of rocks (Table 2). The compositional variations in clinopyroxenes are not as evident as the changes in the anorthite content observed in plagioclases.

The structural formula for metallic oxides was calculated on a basis of 6 or 32 oxygens, depending on the mineral species (ilmenite and Ti magnetite, respectively). 15 points analyzed (> 98%) in 8 crystals distributed between host basalts and pegmatites indicates a composition compatible with ilmenite. TiO$_2$ contents vary between 47.6 to 53.4 wt.% and FeO from 43.1 to 48.2 wt.%. Cr$_2$O$_3$ contents reach up to 0.073 wt.% and MgO content is between 0.9 to 1.7 wt.%. Ilmenite crystals of pegmatites are richer in TiO$_2$ (up to 53.4 wt.%) when compared to those of host basalts. Approximately 13 analyses carried out in metallic oxides of both pegmatites and host basalts define the occurrence of Ti-magnetite. TiO$_2$ ranges from 0.37 to 29.4 wt.% and FeO (total iron) ranges from 57.6 to 92.0 wt.%, with low Cr$_2$O$_3$ contents (< 0.10 wt.%). There is no significant difference between Ti-magnetite from host basalts and pegmatites regarding chemical composition.

DISCUSSION

Co-geneticity and petrogenetic aspects of pegmatites and host basalts

During fractional crystallization processes, the ratio between an incompatible element and a very incompatible one remains constant (Cox et al., 1979; Rollinson and Pease, 2021). In Figure 12, ratios between Zr and Y are constant for host basalts and pegmatites. However, there is Zr enrichment in pegmatites when compared to basalts. Zr and Y chemical behavior indicates that pegmatitic segregations are generated from basalts, by a fractional crystallization process.

In the trace element diagram (Figure 13A), pegmatite samples were normalized by host basalt L24-k2, the sample with the highest mg# value (*i.e.*, the least differentiated one). It is clear that pegmatites are enriched in all

Table 2. Representative EMPA chemical analyses of plagioclase, pyroxene and metallic oxides from host basalts and basic pegmatites of the PIP, in Itaipu. Total Fe is expressed as FeO.

Sample	Basalt (n = 5)		Pegmatite (n = 22)			Basalt (n = 18)		Pegmatite (n = 10)
	L24a-1		L24a-2			L24k-2		L24k-1
SiO_2	51.6	57.3	48.6	53.8	56.4	51.6	55.4	54.1
TiO_2	0.09	0.07	0.04	0.09	0.08	0.09	0.08	0.11
Al_2O_3	29.4	25.9	31.4	28.0	26.4	29.3	27.3	28.0
FeO	0.77	0.66	0.85	0.76	0.50	1.03	0.67	0.73
MnO	0.00	0.01	0.01	0.01	0.01	0.01	0.02	0.01
MgO	0.11	0.02	0.09	0.12	0.06	0.16	0.09	0.15
CaO	13.0	8.17	15.3	11.4	9.14	12.8	10.1	11.2
Na_2O	39.3	6.70	2.79	4.90	5.93	4.00	5.68	4.88
Cr_2O_3	0.00	0.00	0.0	0.00	0.00	0.00	0.00	0.00
Sum	98.9	98.9	99.2	99.1	98.5	99.1	99.4	99.2
Si	9.50	10.4	9.00	9.83	10.3	9.49	10.1	9.85
Al	6.37	5.54	6.85	6.04	5.66	6.35	5.84	6.02
Ti	0.01	0.01	0.00	0.01	0.01	0.01	0.01	0.01
Fe	0.11	0.10	0.13	0.11	0.07	0.15	0.10	0.10
Mn	0.00	0.00	0.00	0.00	0.00	0.00	0.00	0.00
Mg	0.03	0.00	0.02	0.03	0.01	0.04	0.02	0.03
Ca	2.56	1.58	3.03	2.22	1.78	2.52	1.97	2.18
Na	1.40	2.35	1.00	1.73	2.09	1.42	2.00	1.72
Cr	0.00	0.00	0.00	0.00	0.00	0.00	0.00	0.00
Sum	20.0	20.0	20.1	20.0	19.9	20.0	20.0	20.0
Mineral Classification	Labradorite	Andesine	Bytownite	Labradorite	Andesine	Labradorite	Andesine	Labradorite
Ab	23.2	45.1	15.4	30.2	39.4	23.8	35.9	30.3
An	76.8	54.9	84.6	69.9	60.6	76.2	64.1	69.7
Or	0.00	0.00	0.00	0.00	0.00	0.00	0.00	0.00

Sample	Basalt (n = 7)		Pegmatite (n = 1)	Basalt (n = 14)		Pegmatite (n = 6)	
	L24a-1		L24a-2	L24k-2		L24k-1	
SiO_2	0.02	0.11	0.05	0.03	1.73	0.01	0.84
TiO_2	51.9	26.2	51.4	50.6	20.9	53.4	15.7
Al_2O_3	0.02	1.61	0.02	0.06	1.82	0.04	0.72
FeO	45.2	65.2	46.1	46.3	60.2	43.4	70.8
MnO	0.51	0.87	0.66	0.48	1.00	0.93	0.36
MgO	1.46	0.73	1.07	1.24	0.39	1.37	0.45
CaO	0.00	0.00	0.00	0.01	0.22	0.01	0.10
Na_2O	0.00	0.00	0.00	0.00	0.25	0.00	0.02
Cr_2O_3	0.01	0.03	0.02	0.02	0.04	0.01	0.04
Sum	99.2	94.8	99.4	98.8	92.6	99.2	89.1
Si	0.00	0.03	0.00	0.00	0.54	0.00	0.32
Al	0.00	0.61	0.00	0.00	0.70	0.00	0.32
Ti	1.97	6.30	1.96	1.94	5.29	2.01	3.76
Fe	19.1	17.6	19.6	1.98	18.6	1.82	22.9
Mn	0.02	0.24	0.02	0.02	0.28	0.03	0.10
Mg	0.11	0.35	0.81	0.07	0.19	0.10	0.23
Ca	0.00	0.00	0.00	0.00	0.07	0.00	0.05
Na	0.00	0.00	0.00	0.00	0.15	0.00	0.01
Cr	0.00	0.00	0.00	0.00	0.01	0.00	0.01
Sum	4.01	25.3	4.03	4.05	25.9	3.97	27.7

Geol. USP, Sér. cient., São Paulo, v. 23, n. 4, p. 65-85, Dezembro 2023

- 77 -

Table 2. Continuation.

Mineral Classification	Ilmenite	Ti-magnetite	Ilmenite	Ilmenite	Ti-magnetite	Ilmenite	Ti-magnetite
Sample	Basalt (n = 13)		Pegmatite (n = 9)	Basalt (n = 14)	Pegmatite (n = 11)		
	L24a-1		L24a-2	L24k-2	L24k-1		
SiO_2	49.9	50.5	49.9	50.2	50.0		
TiO_2	0.80	0.91	1.12	0.98	1.21		
Al_2O_3	0.60	2.21	2.32	1.77	2.11		
FeO	28.1	11.0	14.1	13.5	13.3		
MnO	0.63	0.24	0.34	0.32	0.33		
MgO	14.1	15.1	14.7	13.5	14.2		
CaO	4.78	18.8	16.2	18.2	17.7		
Na_2O	0.02	0.22	0.23	0.22	0.21		
Cr_2O_3	0.00	0.12	0.03	0.09	0.03		
Sum	99.0	99.1	99.0	98.9	99.2		
Si	1.96	1.90	1.90	1.92	1.90		
Al	0.02	0.09	0.10	0.08	0.09		
Ti	0.02	0.02	0.03	0.02	0.03		
Fe	0.92	0.34	0.44	0.43	0.42		
Mn	0.02	0.00	0.01	0.00	0.01		
Mg	0.82	0.85	0.83	0.77	0.81		
Ca	0.20	0.76	0.66	0.74	0.72		
Na	0.00	0.01	0.01	0.01	0.01		
Cr	0.00	0.00	0.00	0.00	0.00		
Sum	3.99	4.02	4.01	4.01	4.01		
Mineral Classification	**Pigeonite**	**Augite**	**Augite**	**Augite**	**Augite**		
En	30.0	33.7	32.7	29.9	31.4		
Fs	59.8	24.4	31.3	29.8	29.4		
Wo	10.2	41.8	36.0	40.2	39.2		
#mg	0.90	0.98	0.98	0.98	0.98		
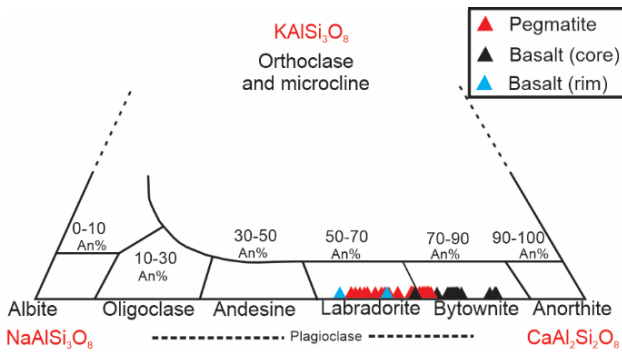
Figure 10. Or-Ab-An ternary classification diagram (Deer et al., 2000) for analyzed plagioclases.

Figure 11. En-Wo-Fs ternary classification diagram (Morimoto, 1988) for analyzed pyroxenes.

incompatible trace elements, with the exception of Sr and Ti, whose values are very close to the values for the primitive host basalt. This enrichment further demonstrates the more evolved character of pe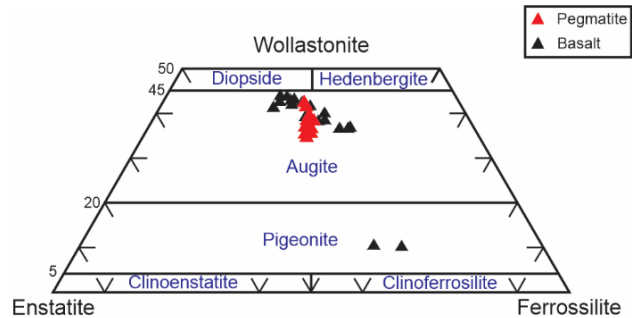gmatitic segregations. The similar contents in Ti are attributed to the occurrence of ilmenite and Ti-magnetite in both groups of rocks. The crystallization of plagioclase in basalts can reduce the Sr content (Deer et al., 2000; Rollinson and Pease, 2021).

The REE diagram normalized by the most primitive host basalt (Figure 13B) exhibits high REE concentrations for pegmatitic segregations and a parallel trend between geochemical signatures of host basalts and pegmatites. It further confirms the hypothesis that pegmatites are fractionated from basaltic melts by fractional crystallization of more evolved, segregated liquids (Puffer and Horter, 1993; Hartley and Thordarson, 2009; Oliveira et al., 2020). Sample L118-b2 represents the most primitive pegmatitic phase when compared to the host basalts while L24-k1, the most differentiated pegmatite.

Fractional crystallization

Major oxides and trace element variation diagrams reveal a linear trend between the groups of studied rocks, which suggests a fractional crystallization model with melt segregation from more primitive, higher mg# rocks (host basalts), resulting in more differentiated, lower mg# rocks such as the basic pegmatites. Trace element geochemical modeling was carried out using the fractionation equations of Cox et al. (1979), with host basalts as primitive rocks (source rock) and basic pegmatites as evolved rocks (residual melt). The exact geochemical compositions of the samples can be found in Supplementary Material 4. Calculations were based on a mineral assemblage composed of plagioclase, clinopyroxene, and Fe and Ti oxides. In order to develop a geochemical model using trace element data and correlate calculated trace element contents (C) to observed trace element contents (O) (C/O), the Rayleigh fractionation equation (Cox et al., 1979) was used.

Trace element comparative calculations demonstrate that it is possible to derive pegmatites from the host basalts. The basaltic liquid commences crystallization shortly after being injected into an inflated pahoehoe-type lava flow.

During the cooling process, after lava flow stagnation, volatiles exsolve from the liquid and tend to concentrate at the lower crystallization front. They subsequently ascend toward the upper parts of the flow, ultimately carrying the melts that formed the pegmatitic segregations (Gomes et al., 2022). As the crystallization process advances, it leads to the formation of a firm crystal mesh (Philpotts et al., 1996; Hartley and Thordarson, 2009) within the basaltic liquid comprised mostly of plagioclase, augite, and metallics. Simultaneously, the remaining liquid becomes progressively enriched with incompatible trace elements such as Y, La, and Ce, which display lower partition coefficients with the solids being precipitated as illustrated in Figure 14. As a result, these elements concentrate in the more evolved liquid and will only be consumed in the
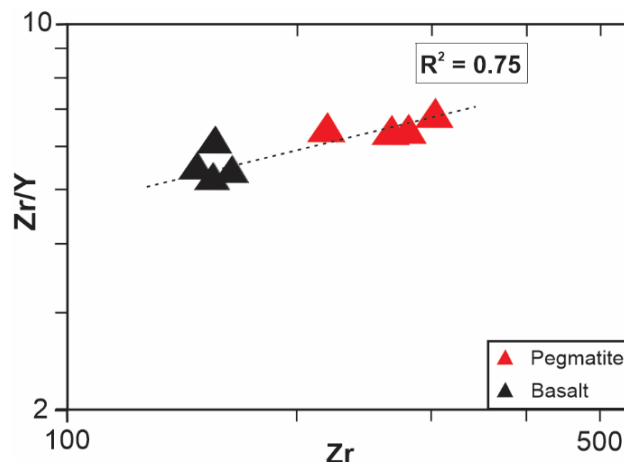

Figure 12. Zr *vs*. Zr/Y diagram for host basalts and basic pegmatites. Note linear trend between both groups of lithotypes.
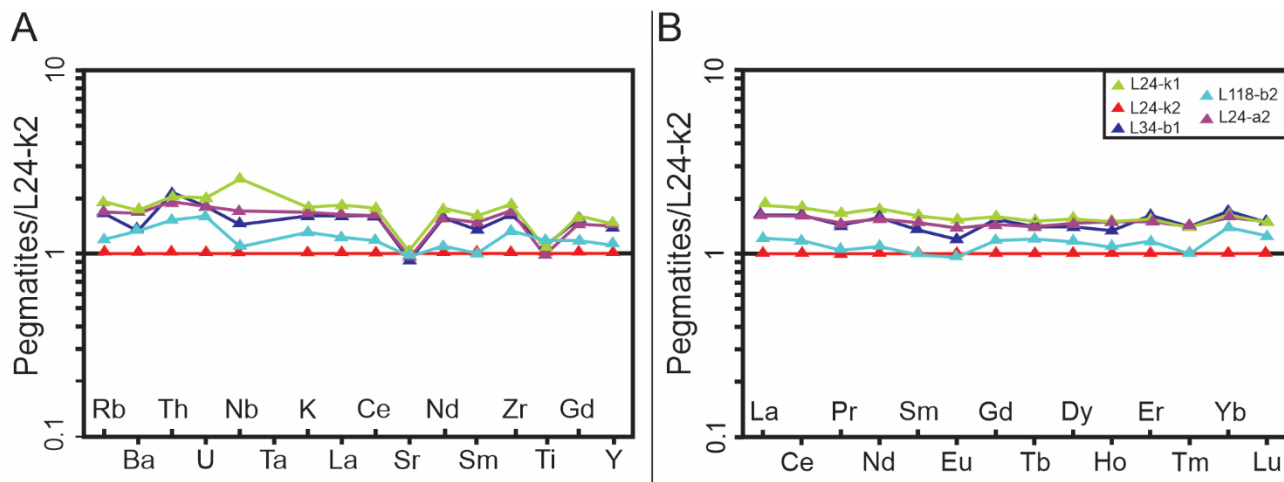

Figure 13. (A) Trace element diagram for basic pegmatites normalized by primitive host basalt (L24-k2). (B) REE diagram for basic pegmatites normalized by primitive host basalt (L24-k2).

final stages of crystallization, after segregation, when the pegmatites are generated. Both the host basalt and the pegmatites contain expressive amounts of plagioclase in their mineral assemblage. As observed in the chemical classification diagram (Figure 10), there is fractionation of a more calcium-rich plagioclase (bytownite) to a less calcium-rich phase (labradorite), which would not generate an anomaly in Eu, as both lithotypes contain plagioclase in a significant percentage. This suggests that Eu is consumed equally during the initial stages of the host basalt crystallization and later, when the pegmatites are formed. The behavior of trace elements during fractional crystallization, based on their compatibility with solids, depicted in Figure 14, demonstrates that the most incompatible elements will remain in the melt, leading to the enrichment of the subsequently segregated liquid.

According to the geochemical modeling of trace elements, the formation of basic pegmatite L24-a2 from host basalt L34-b2 occurs when the basaltic crystal mesh reaches approximately 55 wt.% plagioclase, 35 wt.% pyroxene, and 10 wt.% oxide (ilmenite and/or Ti-magnetite). At this point, Al, Ca, and Mg would have been largely consumed in detriment to K, P, and Na (Figure 6). Additionally, compatible trace elements such as Co and Ni will have been consumed and concentrated mainly in the host basalt (Figure 7).

The melt extraction takes place in direct passage when 50% of the original liquid crystallized, leaving the remaining 50% as residual melt. There is no formation of rocks with intermediate chemical characteristics to these end members. Careful consideration of the crystallization process and the proportion of residual melt is crucial in understanding the formation and geochemical characteristics of basic pegmatites arising from the fractional crystallization of basaltic melts. Thermodynamic modeling of whole-rock compositional data obtained from mafic pegmatites within *pahoehoe*-type lava flows located in Capanema (Paraná) has revealed that the pegmatites were most likely the product of highly fractionated melts that were formed after ~38 – 43% of fractional crystallization of their host basalts (Gomes et al., 2022). Trace element C/O ratios for F = 0.50 are shown in Table 3. Results are near 1.00, showcasing the close correlation between calculated values and measured values. With these results, it is possible to determine that the formation of basic pegmatites is compatible with a fractional crystallization model with host basalts most likely being the source rock (Figure 15A).

The subtle discrepancies in La, Ce, and Sm values (Table 3) are related to the occurrence of residual apatite in the pegmatites. REE partition coefficients for this mineral are very high ($D_{La} = 2.8$; $D_{Ce} = 3.2$; $D_{Sm} = 4.99$), therefore the
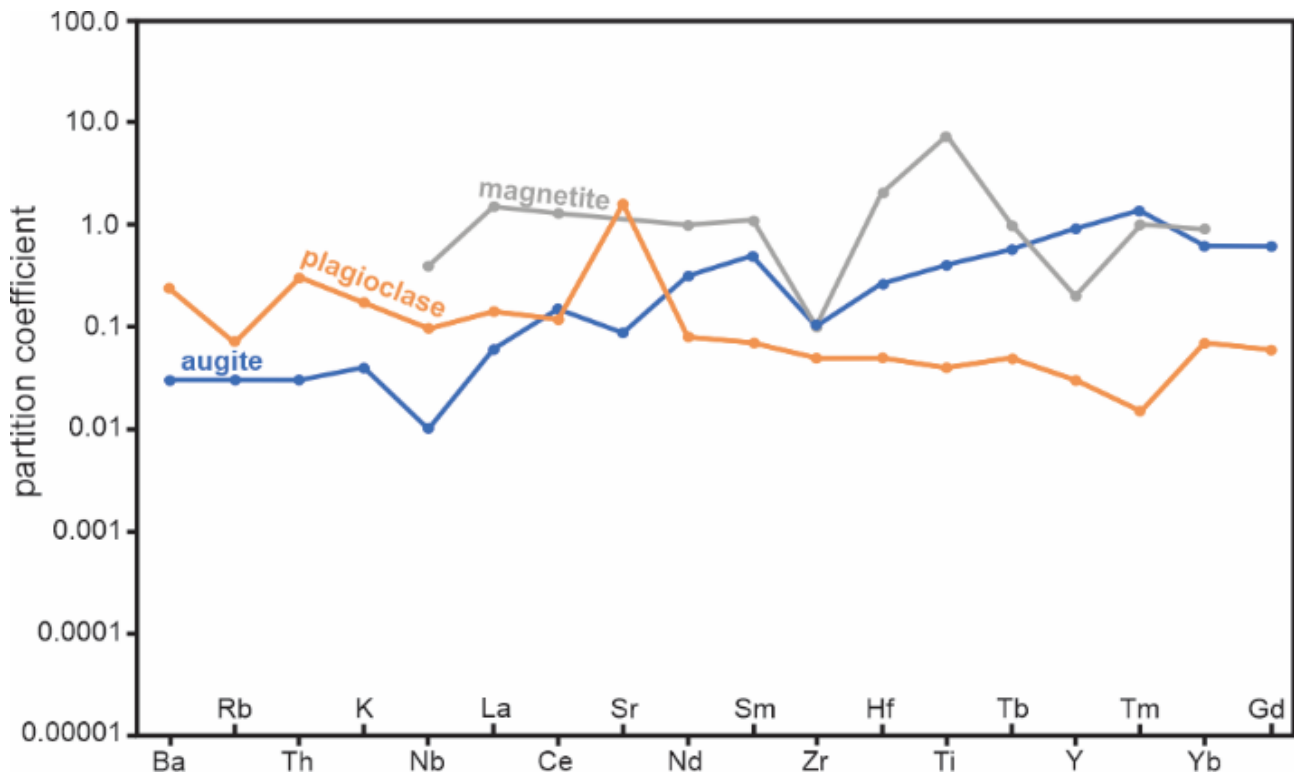

Figure 14. Trace element mineral-melt partition coefficients for the major mineral phases and basaltic melt used in this study. Data from Arth (1976) and Rollinson and Pease (2021).

presence of apatite greatly influences the concentration of these elements in the liquid (Prowatke and Klemme, 2006). Consequently, these elements would be progressively concentrated in the liquid during basalt crystallization (Figure 7) but readily consumed during late-stage apatite crystallization in the pegmatites. The optical identification of apatite in basic pegmatites is not common and therefore, it is possible that its occurrence is in a modal percentage below 1.00 wt.% in these rocks. Hence, LREE would not be consumed during the fractional crystallization of the mineral assemblage observed in host basalts, remaining in the residual melt.

Tentatively, a different melt residual rate was applied to test the consistency of the geochemical model proposed. Initial and final liquid compositions and host basalt mineral assemblage remained the same. For F = 0.40, the residual melt, which would represent pegmatites, would be excessively differentiated and, in this model, would result in the crystallization of pegmatites with a different trace element composition. For this scenario, trace element C/O ratios are shown in Table 3; these values are not compatible with this model of closed-system fractional crystallization. Rocks generated from a residual melt rate of 0.40 would be greatly enriched in LILE-type elements such as Ba, Rb, and K (Figure 15B). Therefore, less differentiation of the initial liquid would be necessary to allow the crystallization of basic pegmatites with trace element concentrations closer to those measured in reality.

CONCLUSIONS

In the western region of Paraná State, in Foz do Iguaçu, basic pegmatites occur within inflated pahoehoe-type basaltic flows from the Paraná Igneous Province. Both pegmatitic segregations and the basaltic flows that host them present very similar mineral assemblage, however their textures are remarkably different, attesting to their distinct development. Host basalts are predominantly microporphyritic in a very fine- to fine-grained, equigranular and phaneritic matrix, whereas pegmatites are medium to coarse-grained equigranular phaneritic. Additionally, specific textures traditionally associated with rapid cooling occur in both pegmatites and host basalts, such as plagioclase bifurcated end features (swallowtail) and very fine, acicular crystals in the matrix. Metallic oxides with skeletal habit and a mesostasis comprised of devitrified microliths are also observed.

The geochemical aspects observed in the studied lithotypes point out to their similar origin, albeit different evolution trends. Host basalts were originated from more primitive melts, giving their higher mg# and lower TiO_2 contents, in stark contrast to pegmatites. Moreover, it is possible to visualize the melt evolution trend from basalts to pegmatites in the Fenner-type variation diagrams that show enrichment in SiO_2, FeO, Na_2O, K_2O, and P_2O_5, opposite to a depletion in Al_2O_3, MgO, and CaO. These trends are in conformity with the geochemical classification of Licht (2018), in

Table 3. Trace element C/O ratios calculated for fractional crystallization of basic pegmatites from residual melts of host basalts.

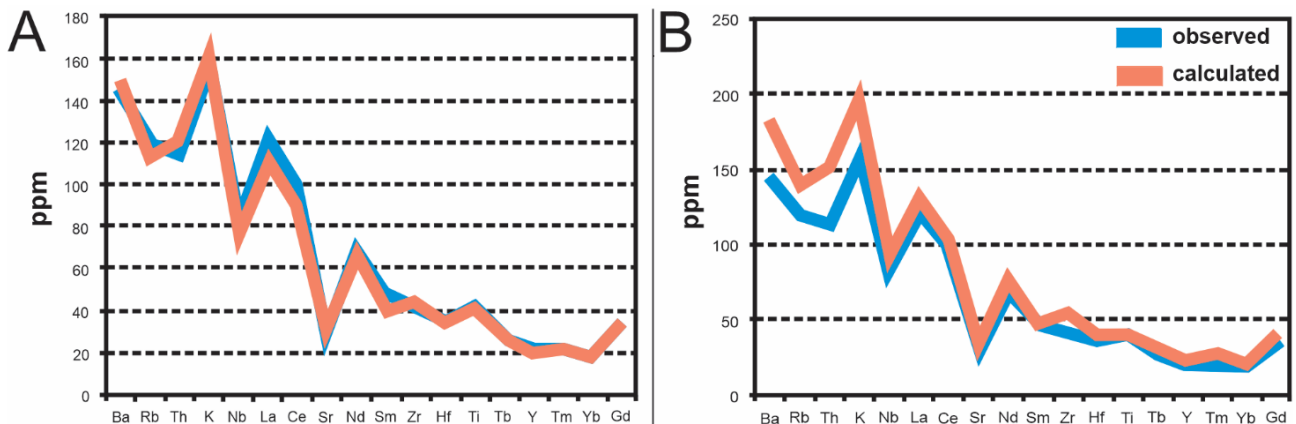| F = 0.50	Ba	Rb	Th	K	Nb	La	Ce	Sr	Nd	Sm	Zr	Hf	Ti	Tb	Y	Tm	Yb	Ga
C/O	1.03	0.94	1.07	1.03	0.88	0.96	0.92	1.08	0.97	0.87	1.06	0.94	0.98	1.04	0.92	1.07	0.96	1.03
F = 0.40	Ba	Rb	Th	K	Nb	La	Ce	Sr	Nd	Sm	Zr	Hf	Ti	Tb	Y	Tm	Yb	Ga
C/O	1.25	1.17	1.33	1.25	1.09	1.13	1.08	1.08	1.14	1.02	1.30	1.10	1.00	1.22	1.07	1.30	1.11	1.22

Figure 15. (A) C/O (calculated *vs.* observed) trace element ratios for a geochemical fractional crystallization model based on residual melt of F = 0.50, for host basalts and basic pegmatites of Itaipu. (B) C/O trace element ratios for a geochemical fractional crystallization model based on residual melt of F = 0.40, for host basalts and basic pegmatites of Itaipu.

which the basalts are classified as type 1 (low titanium and phosphorous contents), while pegmatites (mainly andesi-basalts and trachy-basalts) are classified as types 2, 3 or 4 (displaying varied contents in titanium and phosphorous). The same deportment can also be seen in LILE-type elements, where pegmatites show an enrichment in Ba, Rb, Th, and K in relation to basalts, which is expected in incompatible elements that tend to concentrate in residual (*i.e.* more evolved) melts. Similarly, La/Lu$_N$ ratios range between 5.4 to 6.5 in host basalts and 6.3 to 7.9 in pegmatites, indicating a higher degree of REE fractionation in the former, demonstrating that they are more differentiated and, therefore, more evolved. Although they present different evolutionary paths, the REE signature of all the studied rocks points to a single source rock generating a melt that originated both sets of lithotypes due to the strong parallel trend between them. These characteristics are in agreement with a crystallization model in which pegmatites were generated from more evolved segregated liquids than those responsible for the formation of the basaltic flows.

Finally, the geochemical signatures obtained, such as the ratio between incompatible elements (Zr/Y), indicate that the pegmatitic segregations were generated from host basalts through fractional crystallization and with no intermediate end members. According to the results of trace element geochemical modeling, the fractionation of basic pegmatites initiated with the crystallization of an originally more primitive liquid, generating the host basalts and, at 50% magma crystallization, a residual and more differentiated liquid was segregated, generating basic pegmatites. Melt segregation occurred after a basaltic crystalline framework had formed with a mineral assemblage composed of 55 wt.% plagioclase, 35 wt.% pyroxene, and around 10 wt.% oxides (ilmenite and/or Ti-magnetite).

ACKNOWLEDGMENTS

REFERENCES

Arioli, E. E. (2008). *Arquitetura faciológica da sequência vulcânica e o significado exploratório das anomalias geoquímicas de Elementos do Grupo da Platina (EGP) e metais associados no Sistema Magmático Serra Geral, Estado do Paraná, Brasil*. Thesis (Doctorate). Curitiba: Setor de Ciências da Terra – UFPR. Available at: https://acervodigital.ufpr.br/handle/1884/27955?show=full. Accessed on: Sept. 30, 2020.

Arioli, E. E., Licht, O. A. B., Vasconcellos, E. M. G., Bonnet, K. L., Santos, E. M. (2008). Faciologia vulcânica da Formação Serra Geral na região de Guarapuava, Paraná. *IV Simpósio de Vulcanismo e Ambientes Associados.* Foz do Iguaçu: SBG.

Arioli, E. E., Licht, O. A. B. (2006). Mapeamento Geológico da Formação Serra Geral: Relatório Final das Folhas Cartográficas de Dionísio Cerqueira e Francisco Beltrão. Curitiba: MINEROPAR, Available at: https://rigeo.cprm. gov.br/handle/doc/10439. Accessed on: Sept. 20, 2020.

Arth, J. G. (1976). Behavior of trace elements during magmatic processes - a summary of theoretical models and their applications. *Journal of Research of U.S. Geological Survey*, 4(1), 41-47. Available at: https://pubs.er.usgs.gov/ publication/70162511. Accessed on: Mar 1, 2023.

Bellieni, G., Comin-Chiaramonti, P., Marques, L. S., Melfi, A. J., Piccirilo, E. M., Nardy, A. J., Roisenberg, A. J. R. (1984). High-Ti and low-Ti flood basalts from the Paraná plateau (Brazil): petrology and geochemical aspects bearing on their mantle origin. *Neues Jahrbuch Mineralogie Abhandlungen*, 150, 272-306.

Costa, J. (2015). *Estratigrafia e geoquímica da sequência de lavas da Província Magmática do Paraná na região da Usina de Itaipu (PR)*. Thesis (Doctorate). Curitiba: Setor de Ciências da Terra – UFPR. Available at: http://hdl.handle. net/1884/42082. Accessed on: Sept 30, 2019.

Costa, J., Vasconcellos, E. M. G., Licht, O. A. B., Marzoli, A. (2015). Basic pegmatites in thick lava flows of the Paraná Igneous Province, Itaipu Dam region, Foz do Iguaçu, Brazil. *VI Simpósio de Vulcanismo e Ambientes Associados*. São Paulo: SBG. Available at: https://www.researchgate.net/ publication/283086989_Basic_pegmatites_in_thin_lava_ flows_of_the_Parana_Igneous_Province_Itaipu_Dam_ region_Foz_do_Iguacu_Brazil. Accessed on: Mar 1st, 2023.

Costa, J., Vasconcellos, E. M. G., Licht, O. A. B., Pinto-Coelho, C. V. (2014). Sequência de lavas da Província Magmática do

- 82 -

Geol. USP, Sér. cient., São Paulo, v. 23, n. 4, p. 65-85, Dezembro 2023

Paraná na região de Foz do Iguaçu: Identificação de derrames tipo pahoehoe, rubbly pahoehoe e a'a'. *XLVII Congresso Brasileiro de Geologia*. Salvador: SBG.

Cox, K. G., Bell, J. D., Pankhurst, R. J. (1979). *The interpretation of igneous rocks*. London: Chapman & Hall. https://doi.org/10.1007/978-94-017-3373-1

Deer, A. A. W., Howie, R. A., Zussman, J. (2000). *Minerais constituintes das rochas: uma introdução*. Lisboa: Logmans, Green and Co. https://doi.org/10.1180/DHZ

Dunham, K. C. (1933). Crystal cavities in lavas from the Hawaiian Islands. *American Mineralogist*, 18(9), 369-385. Available at: https://pubs.geoscienceworld.org/msa/ammin/article/18/9/369/536718/Crystal-Cavities-in-Lavas-from-the-Hawaiian. Accessed on: Mar 1st, 2023.

Ferreira, C. H. N. (2011). *Geologia do derrame Salto do Lontra e gênese dos pegmatitos básicos associados, Província Magmática do Paraná, sudoeste do estado do Paraná*. Dissertation (Master). Curitiba: Setor de Ciências da Terra – UFPR. Available at: https://acervodigital.ufpr.br/handle/1884/28823?show=full. Accessed on: Oct 20, 2020.

Gomes, A. S., Licht, O. A. B., Vasconcellos, E. M. G., Soares, J. S. (2018). Chemostratigraphy and evolution of the Paraná Igneous Province volcanism in the central portion of the state of Paraná, Southern Brazil. *Journal of Volcanology and Geothermal Research*, 355, 253-269. https://doi.org/10.1016/j.jvolgeores.2017.09.002

Gomes, A. S., Vasconcelos, P. M., Ubide, T., Vasconcellos, E. M. G. (2022). Magmatic and hydrothermal evolution of mafic pegmatites and their host basalts, Paraná Large Igneous Province, Brazil. *Lithos*, 408-409, 106547. https://doi.org/10.1016/j.lithos.2021.106547

Greenough, J. D., Dostal, J. (1992). Cooling history and differentiation of a thick North Mountain basalt flow. *Bulletin of Volcanology*, 55, 63-73. https://doi.org/10.1007/BF00301120

Hartley, M. E., Thordarson, T. (2009). Melt segregations in a Columbia River Basalt lava flow: A possible mechanism for the formation of highly evolved mafic magmas. *Lithos*, 112(3-4), 434-446. https://doi.org/10.1016/j.lithos.2009.04.003

Irvine, T. N., Baragar, W. R. A. (1971). A guide to the chemical classification of the common volcanic rocks. *Canadian Journal of Earth Sciences*, 8(5), 523-548. https://doi.org/10.1139/e71-055

Jahns, R. H. (1955). The study of pegmatites. *Economic Geology*, 50th Anniversary Volume, Part II, 1025-1130. https://doi.org/10.5382/AV50.25

Janasi, V. A., Freitas, V. A., Heaman, L. H. (2011). The onset of flood basalt volcanism, Northern Paraná Basin, Brazil: A precise U–Pb baddeleyite/zircon age for a Chapecó-type dacite. *Earth and Planetary Science Letters*, 302(1-2), 147-153. https://doi.org/10.1016/j.epsl.2010.12.005

Jefferson, C. W., Hulbert, L. J., Rainbird, R. H., Hall, G. E. M., Grégoire, D. C., Grinenko, L. I. (1994). Mineral Resource Assessment of the Neoproterozoic Franklin Igneous Events of Arctic Canada: Comparison with the Permo-Triassic Noril'sk-Talnakh Ni-Cu-Pge Deposits of Russia. *Geological Survey of Canada*. Available at: https://emrlibrary.gov.yk.ca/gsc/open_files/2789/of_2789.pdf. Accessed on: June 5, 2020.

Jensen, L. S., Pyke, D. R. (1983). Komatiites in the Ontario portion of the Abitibi belt. In: Arndt, N. T., Nisbet, E. G. (Eds.). *Komatiites*. London: George Allen and Unwin. P. 147-157.

Kontak, D. J., De, Y. M., Young, W. D., Dostal, J. (2002). Late-Stage Crystallization History of the Jurassic North Mountain Basalt, Nova Scotia, Canada. I. Textural and Chemical Evidence for Pervasive Development of Silicate-Liquid Immiscibility. *The Canadian Mineralogist*, 40(5), 1287-1311. https://doi.org/10.2113/gscanmin.40.5.1287

Lacroix, A. (1929). Les pegmatitoides des roches volcaniques à facies basaltiques: à propos de celles du Wei-Tchang. *Bulletin of the Geological Society of China*, 8(1), 45-49. https://doi.org/10.1111/j.1755-6724.1929.mp8001005.x

Le Maitre, R. W., Streckeisen, A., Zanettin, B., Le Bas, M., Bonin, B., Bateman, P. (Eds.) (2002). *Igneous rocks:* A classification and glossary of terms: Recommendations of the International Union of Geological Sciences Subcommission on the Systematics of Igneous Rocks. Cambridge: Cambridge University Press. https://doi.org/10.1017/CBO9780511535581

Licht, O. A. B. (2001). *A geoquímica multielementar na gestão ambiental. Identificação e caracterização de províncias geoquímicas naturais, alterações antrópicas da paisagem, áreas favoráveis à prospecção mineral e regiões de risco à saúde no Estado do Paraná, Brasil*. Thesis (Doctorate). Curitiba: Setor de Ciências da Terra – UFPR. Available at: https://acervodigital.ufpr.br/handle/1884/41646. Accessed on: Sept 6, 2020.

Licht, O. A. B. (2018). A revised chemo-chrono-stratigraphic 4-D model for the extrusive rocks of the Paraná Igneous

Geol. USP, Sér. cient., São Paulo, v. 23, n. 4, p. 65-85, Dezembro 2023

- 83 -

Province. *Journal of Volcanology and Geothermal Research*, 355, 32-54. https://doi.org/10.1016/j.jvolgeores.2016.12.003

Licht, O. A. B., Arioli, E. E. (2000). *Projeto de Prospecção Mineral no Terceiro Planalto*. Relatório Interno. Curitiba: Mineropar.

Licht, O. A. B., Arioli, E. E. (2018). *Mapa geológico do Grupo Serra Geral no estado do Paraná: nota explicativa.* Curitiba: Instituto de Terras, Cartografia e Geologia do Paraná (ITCG). Available at: http://www.iat.pr.gov.br/Pagina/Mapeamento-Geologico. Accessed on: May 20, 2021.

Mantovani, M. S. M., Marques, L. S., De Sousa, M. A., Civetta, L., Attala, L., Innocenti, F. (1985). Trace element and strontium isotope constraints on the origin and evolution of Parana Continental Flood Basalts of Santa Catarina State (Southern Brazil). *Journal of Petrology*, 26(1), 187-209. https://doi.org/10.1093/petrology/26.1.187

Marques, S. L., Ernesto, M. (2004). O magmatismo toleítico da Bacia do Paraná. In: Mantesso-Neto, V., Bartorelli, A., Carneiro, C. D. R., Brito-Neves, B. B. (Eds.), *Geologia do Continente Sul-Americano: Evolução da Obra de Fernando Flávio Marques de Almeida*. São Paulo: Beca. P. 245-263. Available at: https://geologia.ufc.br/wp-content/uploads/2016/02/geologia-do-continente.pdf. Accessed on: Apr 15, 2021.

McDonough, W. F., Sun S. (1995). The composition of the Earth. *Chemical Geology*, 120(3-4), 223-253. https://doi.org/10.1016/0009-2541(94)00140-4

Merle, R., Caroff, M., Girardeau, J., Cotten, J., Guivela, C. (2005). Segregation vesicles, cylinders, and sheets in vapor-differentiated pillow lavas: Examples from Tore-Madeira Rise and Chile Triple Junction. *Journal of Volcanology and Geothermal Research*, 141(1-2), 109-122. https://doi.org/10.1016/j.jvolgeores.2004.09.007

Middlemost, E. A. K. (1989). Iron oxidation ratios, norms and the classification of volcanic rocks. *Chemical Geology*, 77(1), 19-26. https://doi.org/10.1016/0009-2541(89)90011-9

Morimoto, N. (1988). Nomenclature of pyroxenes. *American Mineralogist*, 73, 1123-1133. Available at: http://www.minsocam.org/ammin/am73/am73_1123.pdf. Accessed on: Dec 7, 2020.

Oliveira, A. V., Vasconcellos, E. M. G., Licht, O. A. B., Santos, A. M. (2020). Petrography and geochemistry of basic pegmatites of the Paraná Igneous Province, southwest of the Paraná State. *Geologia USP. Série Científica*, 20(4), 79-101. https://doi.org/10.11606/issn.2316-9095.v20-161586

Peate, D. W. (1997). The Paraná-Etendeka Province. In: Mahoney, J. J., Coffin, M. F. (Eds.). *Large Igneous Provinces: Continental, Oceanic, and Planetary Food Volcanism*. American Geophysical Union, 100, 217-245. https://doi.org/10.1029/GM100p0217

Peate, D. W., Hawkesworth, C. J., Mantovani, M. S. M. (1992). Chemical stratigraphy of the Paraná lavas (South America): classification of magma types and their spatial distribution. *Bulletin of Volcanology*, 55, 119-139. https://doi.org/10.1007/BF00301125

Philpotts, A. R., Carrol, M., Hill, J. M. (1996). Crystal-Mush Compaction and the Origin of Pegmatitic Segregation Sheets in a Thick Flood-Basalt Flow in the Mesozoic Hartford Basin, Connecticut. *Journal of Petrology*, 37(4), 811-836. https://doi.org/10.1093/petrology/37.4.811

Piccirillo, E. M., Melfi, A. J. (1988). *The Mesozoic flood volcanism of the Paraná Basin:* petrogenetic and geophysical aspects. São Paulo: Instituto Astronômico e Geofísico/USP.

Prowatke, S., Klemme, S. (2006). Trace element partitioning between apatite and silicate melts. *Geochimica et Cosmochimica Acta*, 70(17), 4513-4527. https://doi.org/10.1016/j.gca.2006.06.162

Puffer, J. H., Horter, D. L. (1993). Origin of pegmatitic segregation veins within flood basalts. *Geological Society of America Bulletin*, 105(6), 738-748. https://doi.org/10.1130/0016-7606(1993)105<0738:OOPSVW>2.3.CO;2

Renjith, M. L. (2014). Micro-textures in plagioclase from 1994 - 1995 eruption, Barren Island Volcano: Evidence of dynamic magma plumbing system in the Andaman subduction zone. *Geoscience Frontiers*, 5(1), 113-126. https://doi.org/10.1016/j.gsf.2013.03.006

Rollinson, H., Pease, V. (2021). *Using Geochemical Data to Understand Geological Processes*. 2nd Ed. Cambridge: Cambridge University Press. https://doi.org/10.1017/9781108777834

Rossetti, M. L., Lima, E. F., Waichel, B. L., Scherer, C. M., Barreto, C. J. (2014). Stratigraphical framework of basaltic lavas in Torres Syncline main valley, southern Paraná-Etendeka Volcanic Province. *Journal of American Earth Sciences*, 56, 409-421. https://doi.org/10.1016/j.jsames.2014.09.025

Santin, S. F. (1969). Pegmatitoides in the horizontal basalts of the Lanzarote e Fuerteventura Islands, Series I. *Bulletin Volcanologique*, 33, 989-1007. https://doi.org/10.1007/BF02597705

Self, S., Keszthelyi, L., Thordarson, T. (1998). The Importance of Pahoehoe. *Annual Review of Earth and Planetary Science*, 26, 81-110. https://doi.org/10.1146/annurev.earth.26.1.81

Self, S., Thordarson, T., Keszthelyi, L. (1997). Emplacement of Continental Flood Basalt Lava Flows. In: Mahoney, J. J., Coffin, M. F. (Eds.). *Large Igneous Provinces: Continental, Oceanic, and Planetary Flood Volcanism*. American Geophysical Union. p. 381-410. https://doi.org/10.1029/GM100

Shelley, D. (1992). *Igneous and metamorphic rocks under the microscope:* classification, textures, microstructures and mineral preferred orientation. London: Springer Dordrecht, 445 p.

Soares, J. S. (2016). *Relações temporais, petrológicas e geoquímicas entre pegmatitos básicos e basaltos encaixantes da Província Magmática do Paraná no Sudoeste do Paraná*. Dissertation (Master). Curitiba: Setor de Ciências da Terra – UFPR. Available at: http://hdl.handle.net/1884/43623. Accessed on: Nov 12, 2020.

Szubert, E. C., Grazia, C. A., Shintaku, I. (1979). *Projeto Cobre em Itapiranga: relatório final* (v. III). Porto Alegre: Companhia de Pesquisa de Recursos Minerais (CPRM), Superintendência Regional de Porto Alegre.

Titon, B. G. (2016). *Modelagem geoquímica de pegmatitos básicos na região de Itaipu, Foz Do Iguaçu - PR*. Monograph. (Bachelor of Science). Curitiba: Setor de Ciências da Terra – UFPR. Available at: http://www.geologia.ufpr.br/portal/wp-content/uploads/2018/10/Bruno-Titon-TCC.pdf. Accessed on: Oct 13, 2020.

Titon, B. G., Vasconcellos, E. M. G., Valore, L. A., Dias, I. A., Bahniuk, A. M. (2021). Mineralogical and physicochemical constraints on the hydrothermalism of volcanic rocks in the Paraná Igneous Province, northwestern Paraná state, Brazil. *Journal of South American Earth Sciences*, 112(1), 103554. https://doi.org/10.1016/j.jsames.2021.103554

Vasconcellos, E. M. G., Licht, O. A. B., Braga, L. S. L., Bittencourt, A. V. L. (2001). Gabros da Bacia do Paraná: Aspectos petrográficos e geoquímicos. *VIII Congresso Brasileiro de Geoquímica; I Simpósio de Geoquímica dos Países do Mercosul*. Curitiba: SBGq.

Viccaro, M., Giacomoni, P. P., Ferlito, C., Cristofolini, R. (2010). Dynamics of magma supply at Mt. Etna Volcano (southern Italy) as revealed by textural and compositional features of plagioclase phenocrysts. *Lithos*, 116(1-2), 77-91. https://doi.org/10.1016/j.lithos.2009.12.012

Waichel, B. L., Lima, E. F., Sommer C. A. (2006). Tipos de derrame e reconhecimento de estruturas nos basaltos da Formação Serra Geral - Terminologia e aspectos de campo. *Pesquisa em Geociências*, 33(2), 123-133. https://doi.org/10.22456/1807-9806.19521

Walker, F. (1953). The pegmatitic differentiates of basic sheets. *American Journal of Science*, 251(1), 41-60. https://doi.org/10.2475/ajs.251.1.41

Wildner, W., Brito, R. S., Licht, O. A. B., Arioli, E. E. (2006). *Geologia e Recursos Minerais do Sudoeste do estado do Paraná - Escala 1:200.000*. Brasília: CPRM. Available at: https://rigeo.cprm.gov.br/xmlui/handle/doc/10439?show=full. Accessed on: Dec 2, 2020.

Wood, D. A., Joron, J. L., Treuil, M., Norry, M., Tarney, J. (1979). Elemental and Sr isotope variations in basic lavas from Iceland and the surrounding ocean floor. *Contributions to Mineralogy and Petrology*, 70(3), 319-339. https://doi.org/10.1007/BF00375360

Geol. USP, Sér. cient., São Paulo, v. 23, n. 4, p. 65-85, Dezembro 2023

- 85 -